Title

Thinking green with 2-D and 3-D MXenes: Environment friendly synthesis and industrial scale applications and global impact

Authors

Saxena, Shatakshi
Johnson, Michael
Dixit, Fuhar
et al.

Publication Date

2023-05-01

DOI

10.1016/j.rser.2023.113238

Peer reviewed

Renewable and Sustainable Energy Reviews 178 (2023) 113238

Contents lists available at ScienceDirect

Renewable and Sustainable Energy Reviews

journal homepage: www.elsevier.com/locate/rser

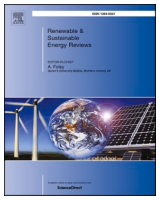

Thinking green with 2-D and 3-D MXenes: Environment friendly synthesis and industrial scale applications and global impact

Shatakshi Saxena [a], Michael Johnson [b], Fuhar Dixit [b], Karl Zimmermann [b], Shreya Chaudhuri [c], Fiyanshu Kaka [d], Balasubramanian Kandasubramanian [d,*]

[a] Centre for Converging Technologies, University of Rajasthan, Jaipur, 302004, India
[b] Department of Chemical and Biological Engineering, University of British Columbia, Vancouver, Canada
[c] Department of Environmental Sciences, University of California, Berkeley, USA
[d] Department of Metallurgical and Materials Engineering, Defence Institute of Advanced Technology (DU), Ministry of Defence, Girinagar, Pune, 411025, India

ARTICLE INFO

Keywords:
MXene nanocomposites
Green synthesis
Defect engineering
Ionic liquid
Supercapacitors
Machine learning
Economic impact

ABSTRACT

MXenes are currently a research hotspot in the field of 2D materials, hinting to revolutionize material technology. Their layered architecture allows for molecular intercalation, defect engineering, and surface band gap functionalization, with applications as diverse as energy storage and drinking water desalination. Its structural and functional integrity has prompted the scientific community to investigate novel compositions in an effort to leverage electrochemical activity, mechanical robustness, flexibility and environmental stability. However, the current synthesis routes present a bottleneck in proposing MXenes as a sustainable material for the future. Therefore, by expanding the reach of synthetic chemistry towards efficient strategies for green production, we present the first comprehensive introspection of the use of green solvents and their impact on material properties during MXene synthesis. This review is an attempt to quantify the intriguing characteristics of MXene nanocomposites by embracing design tools like the 'iceberg model'. To further evaluate the performance of MXenes fabricated using green strategies (such as eutectic etching) we have made an attempt to critically compare them with conventional MXenes by examining surface characteristics, electrochemical analysis, charge transfer mechanisms etc. Conclusively, we aim to instigate concern about the environmental impact of MXene synthesis and instil a multidisciplinary approach to tailor environmentally benign, scalable and efficient MXene derivatives for commercial energy applications. The review provides an immersive account linking UN sustainable development goals with the industrial outlook of green MXenes, it highlights their impact on climate change, potential to build technically advanced economies, low cost production and range of applications.

1. Introduction

To envision a sustainable energy future, we need to explore new energy harvesting materials and derive systems that carry efficient production and storage. The sudden plunge in energy economy is a resulting shockwave of the intractable use of non-renewable fuels to address energy requisites. Last two decades have been witness to the performance of versatile two dimensional (2D) materials and their gradual adoption in the energy sector owing to their excellent conductivity, high capacitance and molecular architecture [1–3]. However, the primary concern with artificial energy harvesters is their inability to control energy dissipation in the form of thermal energy, followed by cyclic instability and industry scale production [4–8]. Despite this, their ordered orientation, refined architectures and the complete transformation in molecular dynamics has motivated researchers to fine-tune existing material properties and search for new materials that offer higher stability and scalable performance [9]. This motive steered Yury Gogotsi et al. to develop a class of sub-nanometer, layered 2D framework of transition metal carbides and nitrides at the beginning of the last decade [10]. This new family of 2D materials known as MXenes are derived from selective etching of their precursor MAX phase, realizing unique characteristics as a result of quantum confined electrons [11]. Despite being in their infancy, MXenes have gained explosive attention among researchers of almost all genres, namely microelectronics [12], tribology [13], battery electrodes [14], conductive inks [15], biomedicine [16,17] and solar thermal desalination [18,19]. Often regarded as 'wonder materials' MXenes are flexible, miniaturized, optically

* Corresponding author.
E-mail address: meetkbs@gmail.com (B. Kandasubramanian).

https://doi.org/10.1016/j.rser.2023.113238
Received 15 July 2022; Received in revised form 13 December 2022; Accepted 6 March 2023
Available online 11 March 2023

Abbreviations

AI	Artificial Intelligence
CNT	Carbon nanotube
CV	Cyclic Voltammetry
CVD	Chemical vapour deposition
DFT	Density functional theory
EE	Electrochemical etching
EM	Electromagnetic
EMI SE	Electromagnetic interference shielding effectiveness
HER	Hydrogen evolution reaction
HF	Hydrofluoric acid
IL	Ionic liquid
ML	Machine Learning
PANI	Poly aniline
PC	Porous Carbon
PCE	Power conversion efficiency
PDA-PEI	Polydopamine-polyethyleneimine
PEG	Polyethylene glycol
PVDF –TrFE	Polyvinylidene fluoride-trifluoroethylene
PVP	Polyvinylpyrrolidone
PT	Photothermal
PW	Parrafin wax
SEM	Scanning electron microscope
XPS	X-ray Photoelectron spectroscopy
XRD	X-ray Diffraction

transparent layered structures with the chemical formula $M_{n+1}X_nT_2$ where M denotes early transition metals, X is a carbon and/or nitrogen, and T is a surface termination functional group [20–23]. Numerous experimentally realizable combinations of M-X, with n and T are employed to build self-assembling hybrids with versatile chemical compositions [24,25]. The ingenious design of MXene structure accords them with a unique intersection of features that are being explored for multifarious energy applications. For instance, studies comparing pseudocapacitive behaviour of various MXene based cathodes like Nb_2C, Ti_3C_2 and Ti_2C in potassium ion capacitors reveal enhanced structural, cyclic stability, low cost and high energy density [26] (see Tables 1 and 2).

To add to the bargain, the range of already explored manufacturing strategies of MXenes like spray coating [27–29], drop casting [30–32], vacuum filtration [33–35], patterned coating [36,37], screen printing [38,39], 3D printing [40,41], elecrospinning [42,43] etc. make them highly suited for industrial scale manufacturing [44]. During the last decade, scientists have understood the emerging constraints with MXene use like aging, toxicity associated with surface chemistry, secondary contamination resulting from degradation in water that need to be considered while substituting MXenes for environment remediation applications [45] other major roadblocks are.

- Rapid oxidation [46].
- Structural degradation (brittleness) [47].
- Loss of conductivity with time [48].

Many studies propose chemical routes to halt oxidation by storing MXenes in inert gas-filled chambers at low temperatures, or redispersing dried MXenes in solvents [49,50]. Despite these, complaints of property degradation over a period of 15 days persist, rendering poor surface conductivity and mechanical strength of the free-standing MXene device [51]. Through this article we address the above-mentioned challenges by reviewing their fundamental causes and propose structural engineering methodologies to overcome the barriers.

Secondly, the state-of-art synthetic approaches suffer from severe human and environmental safety challenges by employing hydrofluoric acid (HF) etching. This makes synthesis complex, entails high purification costs and compromises long term stability, properties [52]. With rigorous work detailing MXene synthesis, there exists an extensive gap between realizing highly efficient MXenes which can be commercialized using safer, milder, environment friendly fabrication tactics [53]. Therefore, we extend our concern regarding the use of toxic precursors for the synthesis of MAX phases and subsequent MXenes. This hindrance stems from the indifference towards the use of strong acid solutions for chemical exfoliation of the A layer of the MAX phase [54]. Moreover, after the fabrication process, the removal and disposal of the by-products pose further environmental risks [55]. To bridge this gap, we have comprehensively compiled the recent developments in green strategies for MXene fabrication and propose potential substitutes of conventional procedures. In the fourth section, we discuss MXenes potential to revolutionize the field of renewable energy by differentiating energy intensive applications of MXenes procured through green synthesis techniques and those fabricated using conventional methods. At the crossroads of choosing renewable energy to avoid long term consequences of fossil fuel combustion, Metal organic frameworks [56] (highly adjustable bandgap, environmental stability), biochar composites [57] (high adsorption capacity, green) and MXenes have emerged as a potential solution by encouraging electro-photocatalysis [58]. Assisting the conversion of greenhouse gases into useful green fuel, these not only open new doors for novel applications but promote renewable energy push despite being a synthetic material.

Finally, we visualize the scope of MXenes in energy applications through employing a design research tool called "*Iceberg modelling*". This model can help to correlate the immediate developments in MXene industry with deeper levels of reasoning and abstraction that are not directly evident (Fig. 1). It is a systematic thinking tool intended to assist in identifying patterns, information and concepts revolving around the subject and identifies how different segments of a system impact and interact with one another. The entire model is divided in four parts: 1. Events-describing the current scenario; 2. Patterns-describing the occurrence of a particular trend; 3. Structure-stating what are the underlying principles associated with the pattern; 4. Mental model-narrating what features and fabrication characteristics might allow for further fine tuning the properties in a desirable manner. Also, it allows us to shift our perspective beyond the available techniques, and achieve better outcomes by integrating multiple technologies.

The last two years witnessed a surge of literature reviews on MXenes, covering fundamental topics like anion [60] and cation intercalation [61], dispersion based analysis, or application specific reports on MXene as actuators [62], EM absorbers [63] etc. Moving this discussion towards a more pressing issue, this review emphasizes the alarming need for greener synthesis methods. While recent reviews covering fabrication and modification techniques of metal organic framework nanocrystals [64] and biochar composites [65] mark as encyclopedia for future developments in their field, similarly this study aims to produce a detailed account of methods that can be adopted for a sustainable MXene industry. We have comprehensively compiled the recent developments in green strategies for MXene fabrication and propose potential substitutes of conventional procedures. Herein, we also attempt to determine the effects of spatial distribution of MXene moieties, functional groups and atomic defects on its electrical and mechanical characteristics. Novelty of the work lies in the selected approach of creating engineering design model to conceptualize industry scale energy applications. This work evaluates the mechanisms involved with intercalation, charge transfer and storage, surface catalysis, sensing etc. and compares them with the performance parameters of HF-etched materials. These procedures can change the trajectory of MXene development as they influence the

Table 1
Details of the various MXene composites with efficiency values in respective application sectors.

MXene	Intercalant	Cyclic Stability	Electrical conductivity and capacitance	Fabrication method	Application	Contribution of MXene on application	Ref.
$Ti_3C_2T_x$	N/A	95% - 10,000 cycles	3352 S/cm and 450 F/cm^3	Spin coating	Photo-voltaic Super Capacitor PSC	Act as electron and hole collector electrode	[20]
88% Ti_3C_2	GO-LC	N/A	72.3 S/cm and 341 F/cm^3	Electrospinning	Textile based storage	Flexible, high conductivity and volumetric capacitance	[95]
$Ti_3C_2T_x$	hydroxyethyl cellulose	82.5%- 10,000 cycles	4.37 S/cm and 68.9C/cm^3	Filtration assisted self-assembly	EMI shielding	Surface group induced multiple reflections and multilayer stacking	[24]
$Ti_3C_2T_x$	V2O5	91.7% 680 cycles	321 mAh/g	Vacuum filtration and Inkjet printing	Electrodes	High Conductivity and mechanical ability increase operating window	[92]
$Ti_3C_2T_x$	additive free	NA	3669.56 S/m	MILD-self assembly	EMI shielding	Availability of oriented charge carries for high ohmic loss	[93]
2% $Ti_3C_2T_x$	NA	NA	Output power density = 3.64 mW/m^2	Electrospinning	Peizo sensing	Improved dipole polarization due to static Electric field force	[94]
$Ti_3C_2T_x$	40% NiO	80% for 90 cycles	13,350 mAh/g	Facile ultrasonication	Li–O_2 battery electrode	High charge density due to abundant active sites	[96]
$Ti_3C_2T_x$	Nickle phosphate	85% for 10,000 cycles	639C/g and 932 W/kg	Hydrothermal method	Supercapacitor electrode	Porous nature and ion tunnels allow fast e– transfer	[97]
$Ti_3C_2T_x$	C–MoS2/CNT	94.6% after 200 cycles	562 mAh/g	One-pot hydrothermal synthesis	Multicomponent electrodes	Large number of electronic coupling states near Fermi level	[98]
$Ti_3C_2T_x$	barium hexaferrite	NA	NA	Tape casting method	EMI shielding	Quarter wavelength attenuation	[99]
$Ti_3C_2T_x$	FeOOH QD/C3N4/ IL	85.2% after 10,000 cycles	391.78 F cm −3	Vacuum filtration	Flexible super capacitors	Overlap of electron cloud of MXene with positive charge of imidazole ring	[100]
$Ti_3C_2T_x$	WO3/hollow graphene	93% after 10,000 cycles	145.2 F g−1 and 752 W/kg	Electrodeposition and drop casting	Asymmetric supercapacitor	Reversible redox kinetics	[101]

Table 2
Comparing the pros and cons of suggested green methods.

Green-MXene synthesis technique	Advantages	Efficiency or Yield	Challenges
Electrochemical etching	In-situ, zero toxic chemical waste, easy tunability of MXene property	Etching time reduced to under 5 h	Dependency on HER efficiency, electrode-electrolyte chemistry, scalability
Electrospinning	Homogeneous properties, flexible films, high surface functionalization, industrial adaptability	7–8 h for spinning	Bead formation, coagulation and needle block
Microwave synthesis	Green, energy conservation, highly effective, reduced time	2 h processing, 30 min exposure	Lack of visible results, determination of exposure time
Ionic liquid and DES as solvents	Environment friendly, easy defect engineering, reduced oxidation of MXenes	50–60% exfoliation within 4 h	Costly precursors
Surface acoustic waves	Ecofriendly, extremely low cost, minimum waste management, limited equipment	12% yield – 40 min time	Yield is low, other MAX phases and non MAX phases need to be evaluated.

industry standards, costs and applications. While emissions, recyclability and cost of non-green MXenes have been discussed in a review that highlights the applications in air purification [66], we structure our discussion by comparing the industrial impact of green MXenes under sustainable development goals, climate change and targets considering energy.

The review translates into the first detailed account of recent advances in green-MXene technology. The state-of-the-art literature envisages the potential of MXene in real-time commercial applications by initiating a consequential discussion of approaching MXene research through divergent perspectives.

2. Structural fundamentals of MXene and its derivatives

MXenes are thought to be conductive, its metal or semi-conductor-like behaviour depends on electrical conductivity, size of the resulting MXene ensemble, defects as well as the surface terminating groups [67]. In this view, due to inter-flake effects (increase or decrease inter-flake spacing and electrical resistance), intercalation might bring an alteration in the electronic properties. This effect was reported to increase spacing between the flakes as well as electrical resistance when H_2O and organic ions were intercalated into $Mo_2TiC_2T_x$ [68]. It was seen that MXenes intercalated with a nitrile group exhibit semiconductor-like behaviour whereas presence of H_2O in $Ti_3C_2T_x$ MXene showcases the inherent metallic properties [69]. Here, the type of functional group needs to be investigated in order to gain an understanding on the exact changes being introduced within the material. Using the difference in electrical conductivity to advantage, researchers have explored semiconductor like titanium carbide MXenes for constructing heterojunction composite when paired with other semiconductor materials [70]. Nemani et al. experimented with double transition metal MXenes by successfully synthesizing MAX precursors (reactive sintering) and layered $M_3C_2T_x$ and $M_4C_3T_x$ (chemical etching) (depicted in Fig. 2) [71]. The accordion like morphology, high entropy and single-phase structure are a result of controlled transition from multiphase MAX to single phase-MXene. The entropic contribution of $M_4C_3T_x$ (−0.2238 eV/f. u.) is higher than $M_3C_2T_x$ (0.1773 eV/f. u. at 1600°C) making it more stable for synthesis. Many theoretical studies revolving around MXenes and its derivatives have highlighted that the control of surface termination

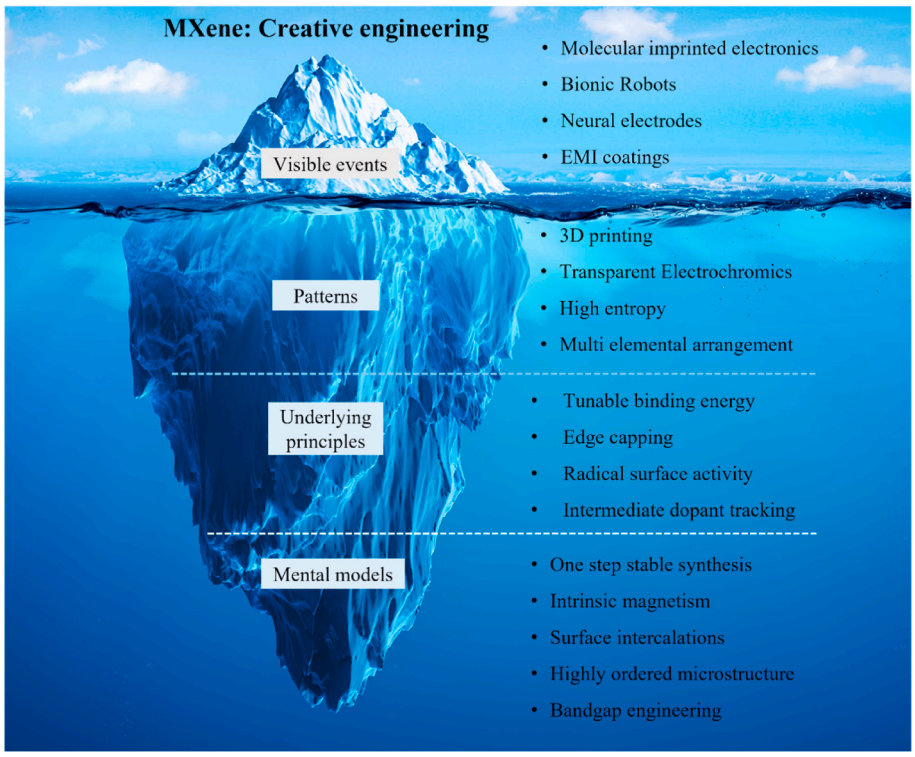

Fig. 1. Design-research perspective of scientific progress: 10 years of MXenes, assumptions (mental models), structure (underlying principles), patterns (trends) and visible events are presented in the form of iceberg model to explain the shift to MXene-based energy intensive systems. Adopted using data depicted in Ref. [10, 11,59].

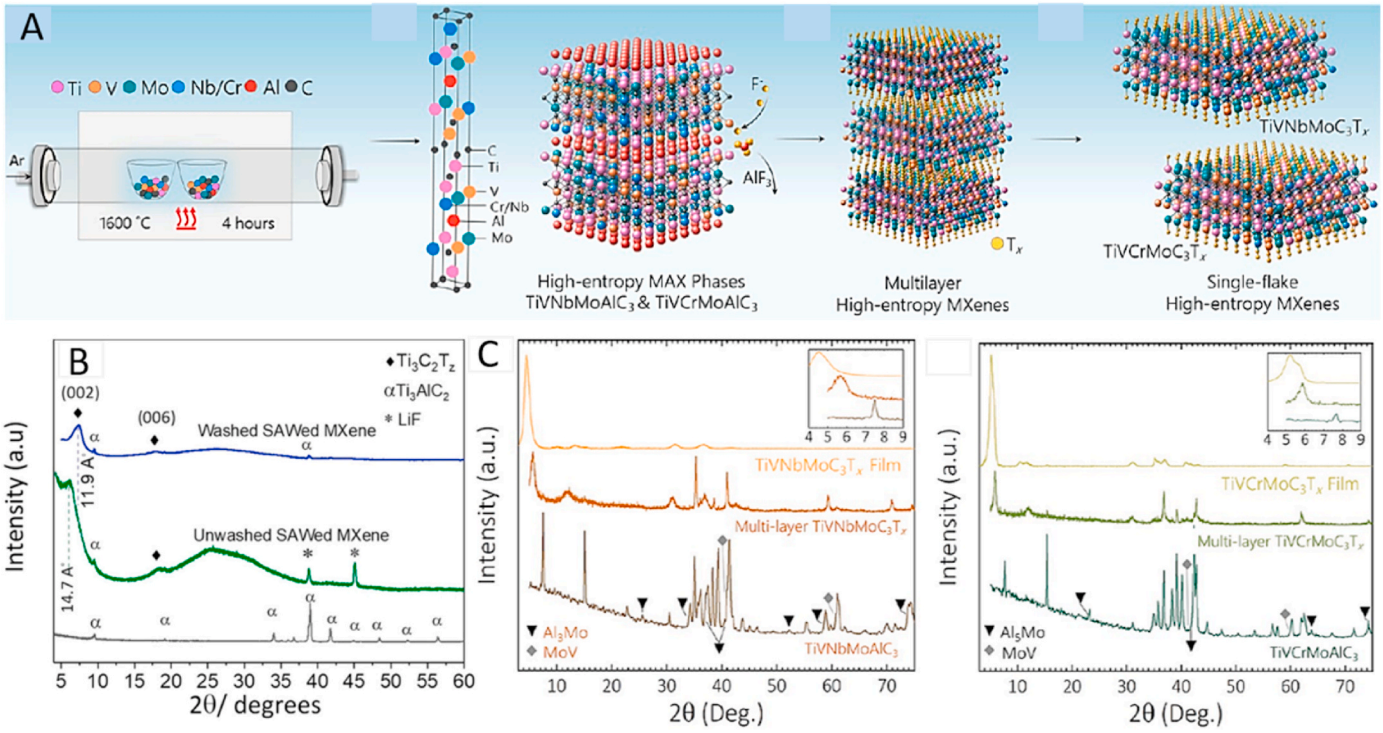

Fig. 2. (A) Schematic depicting fabrication of MAX phase and high entropy MXenes, the different stages show sintering of elemental particles in a tube furnace, MAX phase composed of 4 transition metal elements, multilayer high entropy MXenes formed via delamination using organic intercalants. (B) XRD peaks for Ti_3AlC_2 and freestanding Ti_3C_2 showing decrease in interlayer spacing (14.7–11.9 Å) that confirms the removal of intercalated water layer. Reprinted with permission from Ref. [74] Copyright 2021,ACS. (C) XRD pattern showing changes from MAX precursor to exfoliated MXenes. Inset highlights the shift of (002) peak from MAX to MXene. Reprinted with permission from Ref. [71] Copyright 2021, ACS.

groups, transition temperatures, entropy and metastable phases [72] are vital while synthesizing MXenes [73]. It has been observed that density of states (DOS) at fermi level decreases with surface functionalization signifying a low charge carrier density.

Material properties like crystal structure, twisting angle, stacking phases, and compositional distribution directly influence electrical and magnetic markers of layered materials [75,76]. A depiction of the MXene structure, showing a porous sponge like morphology with innate shielding properties and self-healing behaviour can be seen in Fig. 3. Herein, Ma et al. [77] built a 3-D porous skeleton of self-healing polyurethane to which they spin coated Ti_3C_2 MXenes.

To obtain vertical alignment of carbon (for lower error threshold), liquid nitrogen has proven to initiate formation of cylindrical crystals along the temperature gradient in turn forming an 82% porous, well-aligned layered structure with a density of 0.0006 g/cm^3. Kia Yang et al. [78] explored the use of MXene-based films as a spacer. Herein, carbon nano-tubes (CNT) were used for constructing a highly conductive structure, closely anchoring porous carbon onto the MXene flakes. This increased the contact area between MXene and Porous carbon (PC), facilitating faster electron transportation.. XRD patterns for etched complexes exhibit characteristic peaks at 002 and 006 implying the formation of Ti_3C_2 and removal of Al atoms via etching. The existence of abundant polar groups was confirmed by X-ray photoelectron spectroscopy (XPS) analysis. These negatively charged groups cause repulsion between the flakes in the solution, creating a stable colloidal suspension. The film is highly flexible because of the close fitted anchor of porous carbon onto MXene flakes facilitated by the interwoven CNTs which prevent PC to separate out on bending the film.

2.1. Defect engineering of MXene

The artificially constructed microscopic structure of MXenes allows a wide range of optimization through the incorporation of anchoring sites or defects. Literature shows that the unwanted oxidation of MXenes occurs at the defect sites where carbon is oxidised by the influx of an internal electric field generated by out-of-plane electron movement [79]. This is followed by nucleation of C atom, while the nucleated site attracts intercalation of foreign elements, which results in formation of new and homogenized nucleation sites and reduced reaction time. In a closer study on enhanced visible-light driven photodegradation, N Doped-Carbon supported by Ti was derived from Ti_3C_2 MXene layer [80]. The study explored the drawback of MXene oxidation property into a yielding synthetic approach by manipulating defect chemistry. The complex presented a porous, 2D structure exhibiting rapid electron transport and high stability. The stability of the Ti_3C_2 colloidal suspension is attributed to the hydrophilic and electrostatic repulsion of the adjacent layers. Upon addition of nitrogen containing cationic compounds, self-assembly is induced suggesting a reduction in stacking of u-MXene featuring a wrinkled architecture.

After comparing the existing data with the other reported literature, it was speculated that the HF etching method is more robust and harsher than the LiF/HCl etching and the resulting nanosheets, exhibit large size surface defects. Wang et al. [81] fashioned highly conductive MXene films for moisture driven gradient actuators where the moisture content and deformations in MXene film were correlated with its in-situ preparation. The existence of oxygen-containing functional groups at the terminal site of $Ti_3C_2T_x$ contributed to enhanced hydrophilicity, and presence of –OH ions facilitates hydrogen bonding [82]. Additionally, morphological analysis revealed large size, clean surface and uniform Ti distribution on the MXene flakes with size of about 1.3 nm. This morphology analysis conveys that the fabrication of dense core shell assembly with large molecules occurs due to edge capping of functional groups that assists in maintaining a dense molecular structure.

Ma et al. [83] exploited the crosslinked structure of MXene, demonstrating spontaneous microwave absorption by selectively increasing the temperature at the edges of complex granules, for fast exfoliation and electron bonding. Due to the rapid rise in temperature it was possible to achieve uniform single/few layer assembly with a very small size (2.5 nm in thickness). The ensemble comprised of crosslinked PDA- PEI shell with amino and carboxyl groups yielding hydrophilic, positively charged MXene with interaction between its polar groups and H- bonds. The SEM analysis exhibited a smooth MXene surface relative to the general trend in increased roughness after PDA-PEI coating. EDS studies revealed that oxygen and nitrogen were scattered with uniformity on the surface suggesting a scatter free EM pathway. Li et al. devised an adaptable infrared shielding MXene film with an average emissivity of 0.057 for a broad band ranging from 2.5 to 25 μm [84], the shielding behaviour was reflection governed, however recently V_2CTx and V_4C_3Tx MXenes showing absorption driven EMI shielding (90% efficiency) have also been reported [85].

Fanjie Xia et al. argued that the weak bonds in-between the functionalized metal carbide flakes facilitate an easy exfoliation resulting in thin MXene flakes [86–88]. An interesting feature of this static behaviour is that the functionalized groups not only shield MXenes from oxidation by isolating Ti atoms from oxygen but also blocks ion transport through the surface. Taking into consideration the trap state characteristics, a fresh perspective of oxidation mechanism is proposed. It has been established that Ti vacancy exists as an atomic level defect facilitating the flow of electrons out of plane, resulting in the formation of holes. This initiates creation of an internal electric field prompting carbon nucleation. Now C^{4-} easily loses electrons at trap site, thus promoting oxidation. At this stage, the positive charge at Ti vacancy prompts nucleation of C^0 resulting in amorphous carbon aggregation. With this analysis in hand, it is evident that MXene oxidation is governed by more than a few significant attributes including its exposure to oxygen, functional clusters on the surface and structural defects [89,90]. It is further argued that with control of oxidation kinetics, oxidation progression could be of advantage when fabricating hybrid structures of C-nanotitania. This highlights the importance of defect-sites as nucleation initiators for oxidation. Overall understanding about oxidation phenomenon spurs a new avenue of MXenes in catalysis on the foundation of separation of electrons and holes.

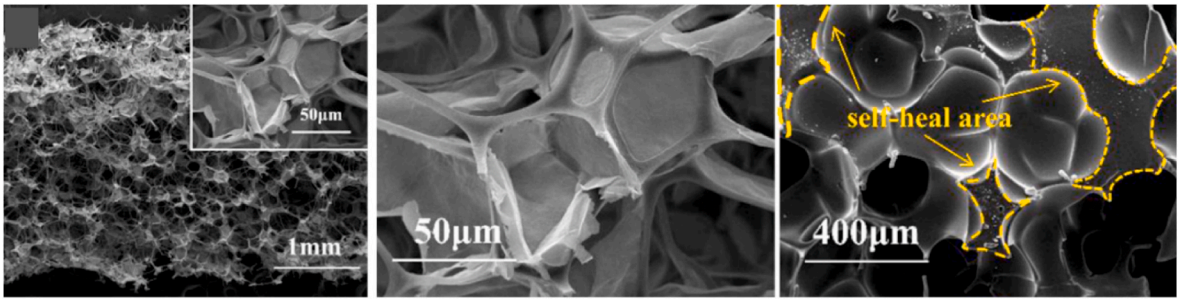

Fig. 3. The scanning electron microscope (SEM) images showing the microstructure of MXene/melamine sponge/polyurethane, showing micro cages for EMI shielding. Adapted with permission from Ref. [77]. Copyright 2021, Elsevier.

A study by Yin et al. [91] on multi-layered structure of MXene associated with PANI-CF fabric use XRD patterns and SEM analysis to understand surface morphology. It was seen that as-prepared MXene sheets possess terminations resulting in a negatively charged surface during the course of etching and delamination process. This enhances their interaction with polar materials without adverse effect on conductivity, indicating potential applications as EMI shielding textiles, flexible electronics and lightweight wearable devices. Upon adhering protonated PANI with MXene, an (EMI) shielded interface is formed via van der Waals forces and electrostatic adsorption. This facilitates continuous and uniform assembly of interconnecting fibers. The dielectric constant signifying the degree of polarization increases from 5.9 to 7.6 with subsequent deposition. The layered assembly benefits from excellent electrical conductivity, high space charge, electronic as well as interface polarization.

So far, we have established that with MAX phase etching, the A layers are removed and replaced by functional groups consequently reducing the binding ability among the metal carbide layer [92–94]. To define the performance niche of MXenes where conventional materials lack efficiency, the following table presents information about various MXene and their principle role for any specific application.

Capitalization on MXenes is possible only when they can be integrated into 3D structures without the use of binders or additives, as by using these compounds high conductivity of MXenes is lost. Zhang et al. [102] endorsed this by referring to the Onsager theory where isotropic to nemantic liquid crystal transitions can occur at critical concentrations of MXene flakes, where critical concentration is dependent on the flake size. The authors relate Onsager theory with an increase in rotational entropy of nematic liquid crystals, which facilitates long range ordering of MXene. Using MXene flakes of 10 μm length and 1.6 nm thickness, this effect was quantified by observing changes in bifringence of Ti_3C_2 inks under polarised optical microscopy, exhibiting monocrystalline structures. On inspecting rheological results, elastic modulus appears to dominate viscous modulus making the ink viscoelastic. These inks can be spun to form fibers, with the highest conductivity achieved using this method was 7748 S/cm, as compared other reported fibers which used binders only achieving <100 S/cm.

2.2. Examining MXene structural fundamentals with artificial intelligence

Recently with the evolution in machine learning (ML) approaches, many have explored the area of AI-driven processes for understanding and predicting new materials and their properties [103]. In this domain, first principle calculations based on evaluating the energies by means of Schrodinger equation are often used to analyse structure and other properties. An attempt by Mu He et al. provides insight into employing ML to evaluate the stability of MXenes with a limited data set [104]. ML approaches associated with materials are mostly data driven where the model is learnt and later established by system. A crucial part of this approach involves selecting effective descriptors that represent chemical information about the material in from of machine interpretable data. On the basis of these descriptors, models established in ML process understand and thereafter predict properties of a material.

Initially, a structured material dataset is prepared followed by feature engineering that evaluates the Pearson coefficient between each characteristic trait. This step is crucial for selecting significant features as inputs and later correlatesinput and output values. The output data is marked as stable or unstable which states stability of MXene. During the study, twenty-five raw attributes with the elemental composition of MXene structure were described. These values were selected as they serve as vital parameters for inorganic materials as per literature. Symbolic regression techniques which analyse models and data sets for compatibility are employed to form new descriptors which are then compared with selected parameters of stability values [105]. The study highlights an interesting fact that a limited data set can also function effectively when dealing with ML approaches saving both computation power and time which would otherwise be needed to process a large dataset.

3. Progress in green synthesis strategies for MXenes

3.1. Challenges of conventional MXene synthesis techniques

To facilitate for the thriving MXene industry, scientists have continuously explored novel strategies of MXene synthesis. In this section, we look at the 10-year journey of developing MXenes from MAX phases using various chemical etchants and understand the effect of variables like pH, temperature etc. e Earliest trials report the use of concentrated hydrofluoric acid (HF), catalysing the reaction between Ti_2AlC and TiC (in an argon environment at 1350°C for 2 h) to obtain multi-layered Ti_3C_2 [106]. However, environmental analysis of HF suggests that it is a systemic toxin, which can lead to penetrating burns or tissue damage in humans apart from being lethal to aquatic life (algae, microbes etc.) [107]. Realizing the need to minimize the use of HF acid, mild etchants like difluoride salts of ammonium, potassium and sodium (NH_4HF_2, KHF_2, $NaHF_2$) were used, but the major drawback here was the 8–12 h long exfoliation time [93,108–110]. hydrothermal synthesis was also carried using NH_4F (150° for 24 h), and NaOH (80°C for 2 h in presence of H_2SO_4), but, the method proved futile when it came to etching of Al molecules from the bulk. Interestingly, the use of NaOH introduced an era of fluoride-free MXenes [111]. In this pursuit, a combination of HCl with Lithium fluoride (LiF) emerged as a promising alternative as it not only reduced the reaction temperature to 35°C but the time dropped from 100 h to under 24 h [53,112]. The challenge with employing HCl and LiF etching remains in the addition of fluorine and chlorine terminations on MXene surface, rendering low specific capacitance, charge storage capacity and the contamination of underground water. This analysis directs us to the demand for MXene synthesis techniques that have a greener impact on the natural ecosystem. Under the term greener, the following strategies can be included; degradation of toxic by-products (through photo and electrocatalysis), minimising the energy consumption of the system (example; microwave heating) and finally the inclusion of green solvents (like water, polyethylene).

3.2. Processing techniques for green synthesis

The following section evaluates the available processing techniques that support the growth of MXene and MXene composites through green methods and builds upon constructive assimilation of the benefits and challenges associated with each approach.

Given that the chemical etching of Ti_3AlC_2 is fundamentally an electrochemical phenomenon where electron transfer takes place from Al to other species, electro-chemical etching could open new avenues for milder and greener synthesis of MXenes. One such selective etching method proposed by Sun et al. uses a unique lithiation expansion-microexplosion mechanism for fluoride free etching of Ti_3AlC_2 anode using a mild electrolyte from Li-ion batteries [113]. Lithiation expansion can be explained by the intercalation of Li ions within MXene interlayers and the simultaneous increase in interlayer spacing on applying a galvanostatic discharge of 0.1 mA. The subsequent ultrasonic treatment of the sample in distilled water leads to a microexplosion reaction in Li_xAl_y alloy that results in the formation of black $Ti_3C_2T_x$ nanoflakes (3 nm in thickness) and evolution of H_2 gas. The delicate balance between etching conditions like solvent ratios, pH and applied voltage was explored by Chen et al. [114]where experiment had a primary goal of replacing hypertoxic HF and other fluorine based solvents with a binary mixture of LiOH and LiCl. This electrochemical setup consists of two Ti_3AlC_2 symmetric electrodes exposed to 5.5 V of constant bias for 5 h. The etching mechanism is attributed to the strong affinity of OH^- and Cl^- ions to Al layers. Similar to the previous study, introduction of Li based electrolytes promotes lithiation and expansion, facilitating delamination of MXene nanosheets. However, this etching setup is

dependent on oxygen evolution reaction as higher amounts of OH^- ions are consumed compared to H^+ ions. It is also reported that the electrolyte pH drops from 11.88 to 10.74 in 5 h of etching supported by the decrease in ionic concentration of Li^+ and Cl^- from 1.783 M to 1.721 M and 1.002 M–0.963 M respectively. The applied voltage in electrochemical etching method can be adjusted to achieve optimal MXene yield, it also affects the morphology of MXene yield making it accordion like (~3 V), layered flakes (~4 V) or amorphous (>7 V) [115]. Similarly, the ratio of chemicals in the solution affects the efficiency of etching, excess of etchants can lead to over-etching forming excess Carbon residue [116]. An entirely in-situ protocol was employed by Li et al. where the electrolyte {LiTFSI + $Zn(OTf)_2$} behaved as an etchant for the MAX phase V_2AlC (cathode) in a closed coin cell [117]. The resulting 2D V_2CT_x flakes retained lamellar morphology, after V–Al bonds of the precursor break due to F^{-1} ions of the electrolyte (OTF^{-1}). Stage two of MXene oxidation forms V_2O_5 particles to which carbon layers interconnect, contributing as a superior matrix benefiting net conductivity. Studies have also reported the use of green electrolytes like methanesulfonic acid/polyvinyl acetate to improve the electrochemical performance of MXene. Liu et al. designed a multistep freeze-thawing process to attain a crosslinked network of PVA in the hydrogel [118]. This 0.5 mm thick electrolyte offers high ionic conductivity = 0.2 S/cm due to reduced stacking of MXenes, increased electrolyte accessibility and freezing point as low as −30°C. Another research reports the use of potassium fulvic acid as an intercalator for exfoliation of MXenes, as it enhances the surface potential (abundant –OH molecules), electrostatic repulsion between $Ti_3C_2T_x$ layers and prolongs the migration path [119]. To study MXenes in neutral aqueous electrolyte Wang et al. suggest the intercalation of $Ti_3C_2T_x$ with dipicolinic acid, achieving very high specific capacitance (353 F g^{-1}) and a 100% cyclic stability for 10, 000 cycles due to adsorption of counter ions by KCl electrolyte and subsequent interlayer hydration of dipicolinic acid [120]. The system promotes electric double layer capacitance and high Faraday capacitance. Phase purity and crystallinity of MXene is estimated by tools like XRD, XPS, SEM, EDS etc. Li et al. identified that phase transition from V_2CT_x to V_5O_2 starts at grain boundaries where the valence state of V^{2+} increases to V^{5+}. Microwave exfoliation carried achieves 100% efficiency within 2 h with a lower shift of (002) peak (9.7°–6.2°) with Ti wt % of 55.19%, reports establish that addition of PFA improves exfoliation efficiency by over 60%.

The cases discussed above use Ti_3AlC_2 precursors for MXene synthesis, but many other MAX phases like Ti_3SiC_2, Ti_2ZnC or even non-MAX phases can be explored for greener routes of MXene fabrication. In one such trial Youbing Li et al. altered the chemistry of Lewis acid $CuCl_2$ molten salt and Ti_3SiC_2 MAX phase, to investigate etching through direct redox coupling at 750°C [121]. During the reaction a volatile $SiCl_4$ compound is formed that behaves as an expansive agent to assist in delamination, while Cu^{2+} and Cl^- are analogous to H^+ and F^- of HF etching system. The as synthesized MXene has a lamellar microstructure and comparable XRD peaks with HF-etched MXene. The reaction follows the following chemistry:

$$Ti_3SiC_2 + 2\ CuCl_2 \rightarrow Ti_3C_2 + SiCl_4 + 2Cu$$

$$Ti_3C_2 + CuCl_2 \rightarrow Ti_3C_2Cl_2 + Cu$$

By contrast Thomas et al. tried synthesizing MXenes by exfoliating a non MAX phase $Mo_6In_2\ C_7$ (non- MAX phases are precursors with a structure of MC_n [$Al(A)_mC_{m-1}$] where A can be Si or Ge, n = 2–4 and m = 3–4) using UV etching [122]. This selective etching technique using concentrated phosphoric acid to obtain Mo_2CT_x after 3–4 h of UV exposure caused lattice rearrangements and oxidation of Mo^{2+} species. This greener approach for MXene preparation is an upcoming trend in the 2-D material industry and efforts can be made to reduce surface impurities like O functional groups by tuning the etching period or chemical concentrations. Yet, there remains much room for optimizing and presenting a scalable, controllable and high purity fabrication method. In this pursuit, Jun Mei et al. [123] proposed a thermal reduction method for fabricating MXene from sulphur comprising MAX phases. Herein, a selective elimination of sulphur from Ti_2SC MAX phase by thermal reduction followed by delamination into 2D MXene architecture was done (Fig. 4). The sulphur layer which is weakly intermediated with metal ion and carbon layers can be etched leaving a weak stack like Ti_2C MXene architecture. The complex records a maximum capacity of 200 mAh.g^{-1} and then saturates at 70 mAh.g^{-1} after 130 discharge cycles. Raising the temperature above 900°C lead to undesirable surface etching and regeneration of Ti_2SC as quantified by the sharp peaks in XRD profile of the sample. The work is a novel approach for green synthesis and is different from other conventional works in two aspects, firstly due to extraction of sulphur from MAX assembly and secondly because of an optimized thermal reduction.

Wang et al. [98] performed electrospinning for different concentrations of MXene/PVDF compositions in order to determine the fiber morphology as well as properties for piezo sensing. Herein, the use of ionic liquid (IL) contributes to achieve a greener process while also reducing oxidation of MXene sheets. In an attempt to make intercalation processeco-friendly Yan et al. [124] employed an in situ approach for ionic electronic coupling, such that IL and HCl acted as in situ etching agents at 54°C. Such type of ion electron coupling confines the 1-ethyl-3-methyllimidazolium ions into MXene interlayers without additional exterior counter ions, and activates surface F groups as well as sub-terminal Ti sites. A three-step synthesis involving the formation of $Ti_3C_2T_x$ powder, IL integrated MXene flakes and HF-MXene flakes was reported. The study highlights that when ions are confined chemically, they facilitate more accessible electro-active sites, a fast electron and ionic transfer in comparison to physical pre-intercalation processes. This can be taken advantage of for applications like supercapacitors, electrochromic devices, batteries etc. The etching conditions studied for various types of MAX phases revealed that MAX & M_2AX phases are relatively easy to etch since they have fewer valence electrons and require milder etching conditions. The energy bargain for Al extraction from multilayered MXenes with nitrogen functionalization is high due to the tightly bound A molecule. Etching processes like wet acid etching, selective etching [125], anodic etching [126], molten salt etching plasma etching etc [127]. fall under ex situ MXene etching synthesis methodology, these result in MXenes with unwanted functional groups. This problem can be addressed by employing in-situ etching, or Chemical vapour deposition bath, these processes also limit harmful chemicals.

3.3. Using green solvents as reaction mediators

Employing aqueous fluoride etchants for selective etching of MXene precursors involves hazardous risk of toxicity which limits investigations [128]. To expand the application of MXenes in water sensitive systems and through an environmentally-sensitive mediator, Natu et al. [126] performed etching and delamination of Ti_3AlC_2 using organic and green propylene carbonate (PC). The resulting MXene structures showed successful intercalation of PC (electrolyte) solvent with an increase in d spacing by 4.5 A°, suggesting that this technique can be carried out in a glove box, in absence of water and shows a potential to be replicated with other MAX phases. Yin et al. [115] modified electrochemical synthesis of $Ti_3C_2T_x$ by replacing toxic HCl electrolyte with room temperature [BMIM] [PF_6] ionic liquid. The as-formed MXene exhibit increased surface defects due to the inherent fluorination, thereby the material possesses higher number of active sites, allowing quick charge transfer. The process can be controlled by manipulating the anodic potential near to 5 V, in turn accelerating electron transfer for rapid etching & fluorination (Fig. 5).

Research has shown that MXenes become chemically unstable and are prone to oxidation in the presence of moisture such as in ambient air, which enormously hinders their potential applications. Ascribed to this view point, Wan et al. [128] demonstrated a robust method to safeguard

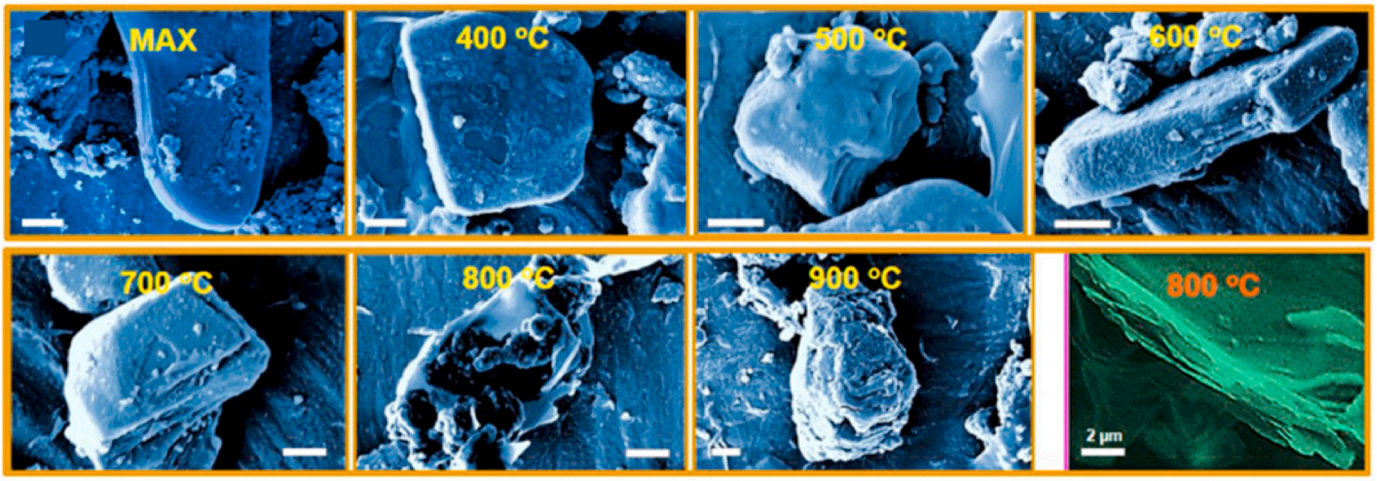

Fig. 4. SEM images showing the morphological evolution with temperature of Ti_2SC MAX phase, suggesting that at an optimal temperature sheet like MXenes are fabricated. Reprinted with permission from Ref. [123]. Copyright 2020, Elsevier.

the 2D layered structure of MXenes from degradation and improve mechanical strength and chemical stability in aqueous media. The study highlights the fact that a higher degree of oxidation and resistivity results in a weaker interface in-between $Ti_3C_2T_x$ sheets and substrates subsequently depleting mechanical strength. It has been reported that rate of oxidation depends on MXene lateral size and a reduction in lateral size speeds up degradation which can be mitigated by employing organic solvents [130,131].

Evaluating the photothermal aspect of $Ti_3C_2T_x$, Cheng et al. [132] explored its applicability as an ink complex with ionic liquid. 1 g Ti_3AlC_2 was added slowly to evade overheating the solution and then the mixture was kept for some time to fully remove elemental Al followed by washing, centrifugation and finally freeze drying at −60 °C. It was also argued that due to the presence of PEI, polar groups got secluded at the interface of $Ti_3C_2T_x$ retaining stable performance of PEI based chip. PEI is added so as to impart a positive charge to polymer and neutralize the negative charge of $Ti_3C_2T_x$, thus avoiding aggregation on addition of IL. SEM, TEM analysis revealed an enhanced rough structure facilitating a diminishing reflection of incident light promotes photothermal conversion. This semi metallic property was seen to induce local surface plasmon resonance amongst $Ti_3C_2T_x$ and incident light resonant wavelength, which suggests that the final product is highly stable and efficient.

A study by Hongran Zhao et al. [133] revolved around tailoring a reliable strategy for preparing air-stable and oxidation-resistant $Ti_3C_2T_x$ MXene sheets via non-covalent functionalization of ILand MXene sheets. MXene were prepared combining Ti_3AlC_2, HCl (30 mL of 9 M) and LiF (3 g) then treating the obtained assembly with 0.5 M IL aqueous solution. The resulting assembly was non-volatile and had enhanced solubility with environmentally-friendly properties as the fluoride percentage in MXenes is lowered. An interesting aspect of the reaction kinetics is that IL acts both as a stabilizer and an intercalant, accelerating MXene phase exfoliation. Further analysis revealed excellent compatibility of the hybrid with water and confirmed that IL plays a crucial role not only in promoting exfoliation of MXene sheets but also in increasing its dispersion in water. Zeta potential analysis provides insights regarding the dispersion of nanosheets and it was seen that value of unmodified MXene nanosheets decreased drastically with time but in case of IL hybrid, it remained stable. It has been previously reported that MXene sheets are prone to oxidation impeding their longevity. In this pursuit, the study by Hanqing Lin et al. [134] where kinetics involving deep eutectic solvent (DES) was explored for greener synthesis. Both eutectic solvents and DES can be considered as environmentally benign reaction media, because of the easy tailorability, biodegradability and low cost. Firstly, a liquid membrane anchored by $Ti_3C_2T_x$ laminate aided by ChCl-EG DES over the nanoslit in between MXene layers [135]. The presence of adequate functional groups at the interface of MXene results in strong hydrogen bonding with DES ensuring affinity in MXene framework and overall stability. Hydrogen bonding can be attributed to impairing of cation anion bond resulting from changes in hydrogen bond network. Further, carbon dioxide mixed with either nitrogen, hydrogen or methane was used to explore the carbon dioxide selectivity mechanism and its potential as a separation system for CO_2.

Another interesting study was reported by Jeonghui et al. highlighting the significance of DES in the reaction kinetics for fashioning more stable and cleaner MXenes [136]. Here, DES was used as an inert anti-oxidant dispersion medium to limit MXene hydration in water and hence adds long term chemical stability. This averts dissemination of oxygen which would have otherwise caused oxidation of MXene. It was also argued that DES in polarized form could act as a viable intercalant for delamination of MXene. Because of the presence of H bond accepting and donating molecules in DES having robust interface with MXene surface, it acts as an excellent antioxidant. On comparing the oxidation effect on DES and organic solvent by adding 10 wt% DI water in each case, it was concluded that DES infused MXenes were able to uphold their oxidative stability whereas MXene dispersed in organic solvent exhibited oxidation under similar conditions.

Wu et at [137]. also explored DES as greener materials for MAX phase treatment, using an oxalic acid & choline chloride precursor is relatively less dangerous and exhibits good solubility when treated with MXene. The DES -MAX environment promotes in situ production of etching agents and the intercalation of choline cations. Increases in interlayer d-spacing improves lithiation kinetics of the overall material. Furthermore, life cycle assessment of DES reveals potential reusability and recyclability even on industrial scale. It has been proven to be a safe, low-cost preparation strategy for industrial/commercial grade MXene. A study conducted by Zhang et al. reports use of a eutectic mixture of $NaCl/ZnCl_2$ to etch Ti_3AlC at 550°C for 5 h [138]. The obtained Ti_3CCl_2 MXene showed mesoporous growth with a pore diameter ranging between 3 and 4 nm (dependent on the concentration of NaCl – 60% mole fraction). Herein, a redox reaction occurs between $ZnCl_2$ and Al producing $AlCl_3$ (volatile) leaving structural defects like pores. These defects are reinforced as NaCl crystals preventing collapse of the structure. This method is superior compared to HF-MXenes because the high temperature treatment prevents generation of O_x terminations and ensures complete CL functionalization. Moreover, the inherent one-step etching secures an ordered distribution of elements in the core with low electronegative shell made of Cl ions and strongly electronegative

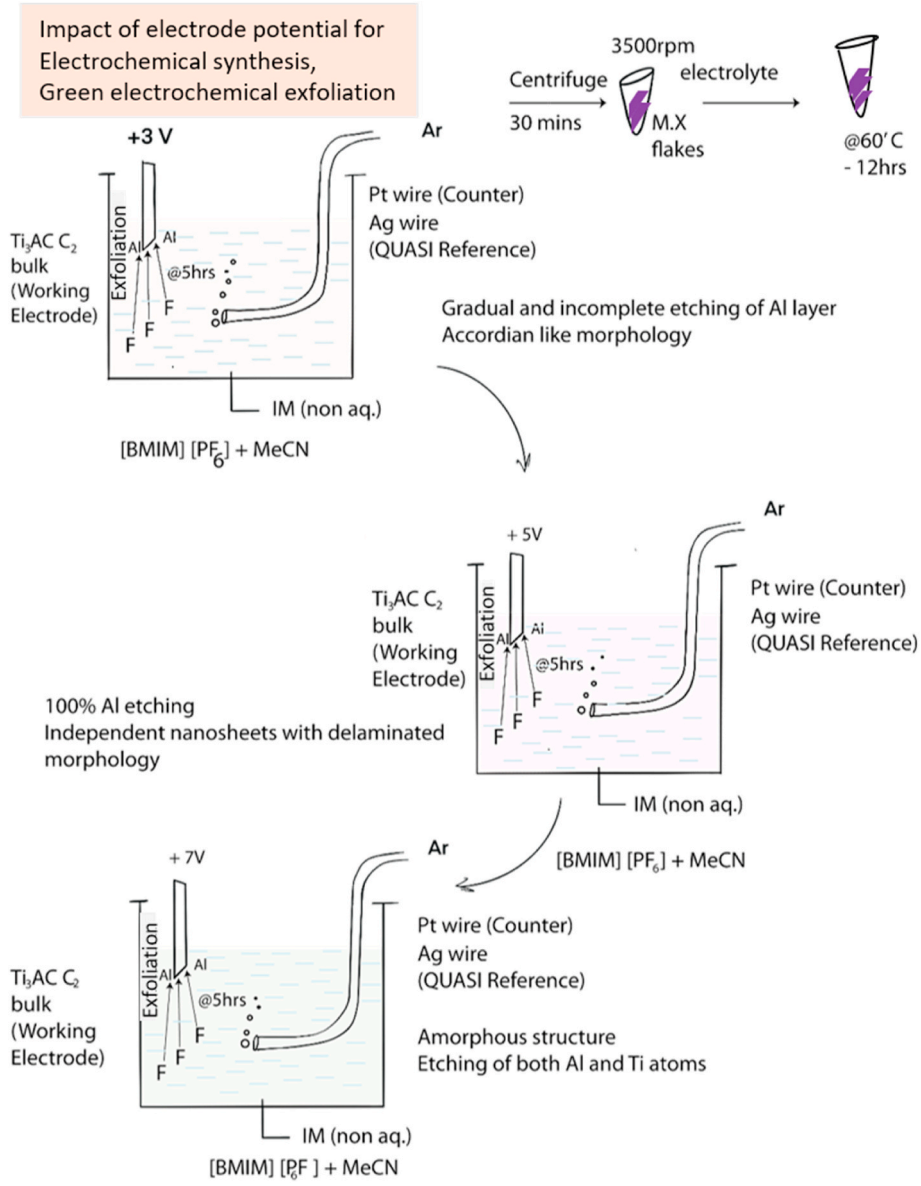

Fig. 5. Studying the dependence of bias potential on etching degree and structure of MXenes using ionic liquid electrolyte to effectively produce greener $Ti_3C_2T_x$ MXenes, redesigned from information given in Refs. [115,129].

core that high density electron clouds. Ghazaly et al. introduce another single step methodology by exploring the world of surface acoustic waves to induce nonlinear electromechanical coupling for selective etching of MAX phases [74]. The localized Rayleigh waves ($10^{8\ -2}$) induce polarization and exciton transport in the layered material while evanescent electric field leads to production of free radicals that ultimately reduce pH thus facilitating dissociation of LiF (faster reaction kinetics) and depleting in-situ HF. To further understand the effect of green synthesis routes on surface charge properties of MXene composites, zeta potential values were analysed (Fig. 6). MXenes generally exhibit very low values of zeta potential (negative values), however chemical etching leads to an increase in negative zeta potential (compared to pristine MXene). In contrast, inclusion of green techniques synergistically assists in lowering the zeta potential values below −30 mV. This can be attributed to the presence of flexible terminations, that minimize particle aggregation. These values also indicate superior degrees of colloidal stability, due to strong electrostatic repulsion between charged particles. For example, if the potential values are negative MXenes flakes remain afloat at neutral pH, this is because the negative surface charge (termination groups) increases with increase in pH [139]. This trend indicates high electrostatic repulsion between MXene layers and can be further analysed to evaluate surface chemistry and adsorption mechanisms. Ultrathin $Ti_3C_2T_x$ are reported to follow the Donnan effect (rejection of negatively charged impurities is high) where for a wide range of pH (3–10) it exhibits a negative zeta potential whereas the HF– $Ti_3C_2T_x$ exhibit positive surface charge at low pH [119]. Zeta potential can be further studied to understand time dependent surface charge transitions [136].

4. Comparing the performance of green fabrication mediated MXenes with conventional MXenes in industry

Among 2D materials MXenes have emerged as a potential species when it comes to factors, like availability of environmentally benign synthesis and post-processing techniques. Now, let us see if these green-MXenes can be applied to solving real-world challenges in energy and energy-mediated fields. The properties like surface functionality, flexible terminations, high selectivity, mass manufacturability and low-cost

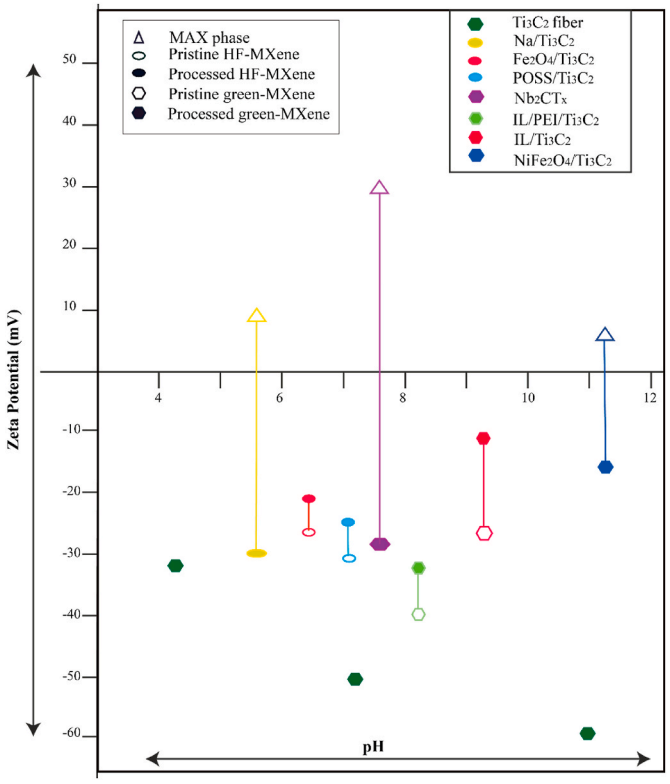

Fig. 6. Comparing the zeta potential values of MAX phases, HF- MXenes and green MXenes suggests that post-processing increases the zeta potential value compared to pristine MXenes, and green-synthesis mediated MXenes have more negative zeta potential values than HF-MXenes.

make MXenes and MXene composites suitable in various industrial sectors. These include anode materials, ion storage batteries, supercapacitors, electrochemical sensors, photocatalyst, separation membranes etc. Their performance has shown comparable results to other 2D material systems including graphene or CNTs. In this section, we highlight the applications of green-MXenes, discuss their performance parameters (capacitance, surface area etc.) and further evaluate methods that show promising outcomes at the industrial scale.

4.1. Solid state electronic applications

Herein, we compile the examples of green-MXenes explored as anodes, batteries or supercapacitors and compare the results of electrochemical studies to identify various surficial and interfacial mechanisms governing the kinetics. Environment friendly techniques like UV assisted synthesis or Lewis acid treatment have become extremely popular in the past few years for MXene fabrication. These can be readily scaled up for industrial bulk production of MXenes from MAX as well as non-MAX precursors. Generally, the most concerning challenge with HF- etched MXenes in non-aqueous electrolytes is the sequential intercalation/deintercalation of Li^+ ions resulting in the need of a high operating potential at the cathode [140]. This large difference in the operating potential window was targeted by Li et al. in studying the CV characteristics of $Ti_3C_2T_x$ fabricated using molten salt of $CuCl_2$ [121]. The electrochemical signature reveals that during the cathodic scan Li^+ intercalation occurs between MXene layers because of the change in oxidation state of Ti (0.4 electrons transferred per atom), whereas during anodic scan a mirror-like profile appears due to the loss of Li^+. Moreover, a solid electrolyte interphase layer is also formed during reduction phase that blocks the co-intercalation of solvent molecules. Thus, molten salt- $Ti_3C_2T_x$ operates within a potential window of 0.2–2.2 V, revealing a pseudocapacitive charge storage mechanism with a discharge capacity of 205 mAh g^{-1} at 0.5 mVs^{-1}. Also, the absence of surface OH groups, helps in decreasing the charge-transfer resistance to as low as 25 Ω cm^2 indicating towards diffusion limited kinetics. Considering that exposure to electric field can make the etching process rapid and efficient Sun et al. further analysed the electrochemical performance of as prepared $Ti_3C_2T_x$ samples [113]. The CV curves were similar to those obtained in conventional double layer capacitors, forming rectangular shapes with zero redox peaks. Electric field assisted lithiation and expansion results in the introduction of oxygen rich attack sites and ultrathin morphologies, both enhancing capacitance character. The sample records a specific capacitance of 338 Fg^{-1} at 0.5 Ag^{-1}.

Apart from electric field other parameters like ultrasonic treatment or thermal reduction have also been examined to etch MXenes [141]. Mei et al. investigated the potential of thermally reduced MXenes that possess high density distribution of Ti and C species along with some O terminations, for anode materials [123]. During the etching process few graphitic carbon layer by-products were also formed, facilitating in rapid charge transfer, faster ionic diffusion and lowered internal resistance. The CV investigations were carried under an operating potential window of 0–3 V, revealing successful intercalation of Li^+ ions within Ti_3C MXene. The complex records a maximum capacity of 200 mAh.g^{-1} and then saturates at 70 mA h.g^{-1} after 130 discharge cycles. This reduction in charge storage capacity can be attributed to the presence of unstable solid electrolyte interface on the surface of active MXene electrode.

In a recent study Chen et al. fabricated high efficiency $Ti_3C_2T_x$ flakes comprising of 2–3 layers of $Ti_3C_2T_x$ of 3.9 nm thickness [114]. These show high stability compared to HF-MXenes that oxidize when dispersed in an aqueous medium for 15 days at 25°C. The material was characterized using a Swagelok cell configuration in a 3 electrode setup, wherein $Ti_3C_2T_x$ displayed a redox-type CV curve with a maximum specific capacitance of 286.2 F g^{-1} at 5 mV s^{-1}. It supports fast charge transport kinetics as reflected by the shift in anodic and cathodic redox peak potential values from −0.26 to 0.222 V and −0.305 to-0.337 V respectively [142,143]. The electrode offers high areal and volumetric capacitances of 1.39 F cm^{-2} and 1160 F/cm^3 respectively, which is higher than HF etched MXene/reduced graphene oxide composite (0.049 F cm^{-2} and 490 F cm^{-2}) [144]. Upon assembling the electrochemical etching (EE) - $Ti_3C_2T_x$ as cathode with Poly vinyl alcohol (PVA)/$ZnSO_4$ in a flexible zinc-ion capacitor, the system shows linear galvanostatic charge/discharge curves suggesting a capacitive charge storage behaviour (Fig. 7).

Moving forth, let us consider MXenes prepared using eutectic solutions for applications as battery anodes, $Ti_3C_2Cl_2$ peaks show non-diffusion limited charge storage mechanism as quantified by its ability in accommodating high current cycling [59.4% at 1 mV s^{-1} to 89.7% at 10 mV s^{-1}]. The meso-porous structure not only assists in improving the reaction kinetics it also promotes high Li^+ diffusivity due to the lowered diffusion barrier [138]. Besides, the rapid Li^+ intercalation due to steric from Cl^- terminations adds on in improving the electrochemical performance with a low activation energy of 0.2 eV $Ti_3C_2Cl_2$ MXene is structurally stable for practical long term cycling as suggested by the 89% retention capacity after 100 cycles. The reported method is superior than HF synthesized MXenes [145] as the latter gives a Li-ion storage capacity of 146 $mAhg^{-1}$ compared to the 382 $mAhg^{-1}$. This improved capacitance can be attributed to low ion transport resistance, short diffusion paths and structural stability. Also, the auxiliary migration channels through Cl atoms along with the hopping migration of Li ions on top of Ti and C atoms contribute in battery applications where high power charge-discharge cycles are needed.

Hence, we can predict that there is a high industrial potential of MXenes developed using green synthesis strategies. The examples discussed reveal comparable electrochemical performance, rather most of the green-MXenes allow fine-tuning of the involved kinetic mechanisms. The systems also show high cyclic stability and therefore can be used in real-time energy storage setups. The next-stage is to evaluate the

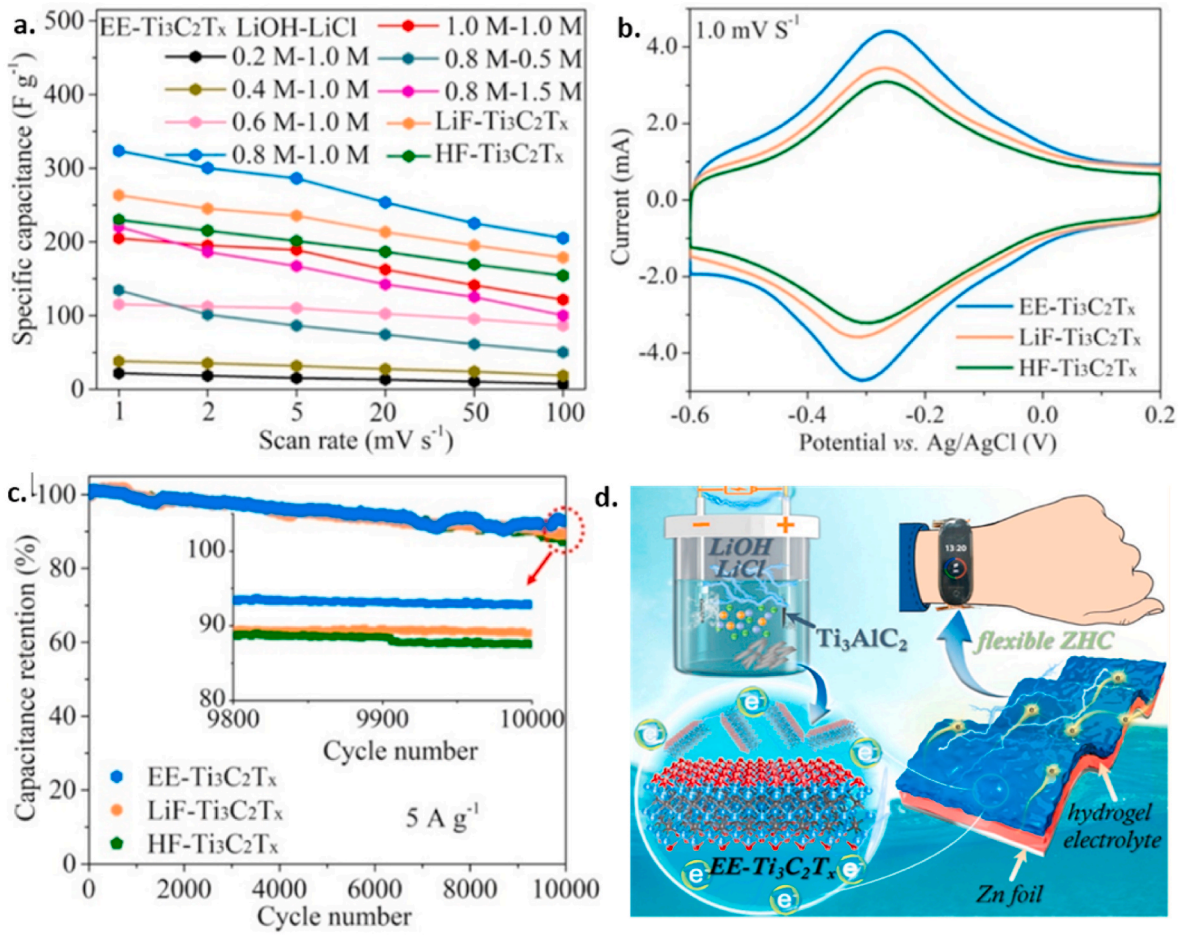

Fig. 7. (a–c) Illustration of electrochemical analysis comparing HF-MXenes, LiF-MXenes and EE-etched MXenes, the figure (d.) highlights the application scope of green MXene in flexible electronics. Adapted with permission from Ref. [114]. Copyright 2022, ACS.

reproducibility of the material and analyse the performance in extreme temperatures of the order −40°C where the aqueous electrolyte freezes affecting overall performance.

4.2. Translational research and applications

Swapping HF-MXenes with green solvent mediated MXenes solves the biggest problem associated with the toxicity of fluorine based materials and harmful by-products. Throughout the review we have seen that much work has been channelled towards adopting green chemistry approaches for MXene fabrication. However, we know that there is a lot of scope in using nature derived methods for synthesis of environmentally benign materials. Following this suit Zada et al. made an attempt to obtain Vanadium carbide (V_2C) MXenes from V_2AlC through algal extraction method [146]. V_2C is one of the least stable MXenes, prone to oxidation and low yield, therefore, an eco-friendly method with high yield ratio is proposed. During the reaction, organic acids of the algal mixture attack V–Al sites, driving the intercalation of bioactive molecules, further accelerating efficient cleavage and delamination.

The calculated yield of the nanosheets was around 90%, with V_2C exhibiting strong absorption band in the near infra-red window. Moreover, cytotoxicity analysis proves that even at high concentrations (200 μg mL^{-1}) algal extraction mediated nanosheets have negligible toxicity for MCF-7 cells. So, these biocompatible V_2C MXenes are evaluated for applications in photothermal (PT) therapy and the efficiency is compared with that of other reported PT agents. The photothermal conversion efficiency of V_2C MXene is about 48%, which is significantly higher than HF-produced Nb_2C MXene (36.4%). After understanding the efficacy of this system in-vitro, in-vivo studies were conducted by treating cancer cells with V_2C NS (10 mg/kg), and exposing them to 808 nm laser for 10 min, the results demonstrated effective cell-death with complete ablation of tumor in 12 days. Thus algal extraction can be scaled up and employed to extract bulk-MXenes from different precursors. The as obtained material can be directly used for biomedical applications because of its bio-derived, non toxic components. Excessive surface fluoride residues due to HF etching leads to its in-vivo release and cell-lysis, therefore we need fluoride free electrochemical etching routes. Song et al. successfully synthesized transparent, ultra-thin Nb_2CT_x with hexagonal microstructure using 3D electrode thermo assisted EE technique, during the reaction the Al in Nb–Al bond is replaced by lighter atoms resulting in abundant hydroxyl groups on the surface [147]. The material shows photoabsorption in NIR spectra as well as its anisotropic electron transport behaviour and a large surface area (35.3 m^2 g^{-}) all of these properties are beneficial for efficient and rapid biosensing platform. A Nb_2CT_x/acetyl cholinesterase biosystem was assembled for organophosphate detection [148]. It shows higher sensitivity compared to O-functionalized MXenes due to the presence of inherent metallic properties and near zero band gap. Moreover, in HF etched Nb_2CT_x, the gradual decrease in anodic current is attributed to the formation of NbO_x species [149]. The fabricated biosensor offers real time detection, enhanced enzyme activity (response signal increases from 0.39 μA to 3.72 μA) due to the presence of AChE.

MXenes can also be engaged in optical sensing applications because of their high conductivity, adjustable molecular size and electrochemiluminescence (ECL). Nie et al. prepared MXene quantum dots (MQD) using microwave heating method in 15 M NaOH environment at

180°C~60 min [150]. After washing and decanting the pre-treated QDs were irradiated with microwaves for another hour at reduced temperatures of 110°C and 200°C. Herein, band-gap engineering was performed to maintain the difference in energy bad gaps (E_g) of surficial and core MQDs (ranging between 225 and 330 nm), such that E_g surface is smaller than E_g core to ensure rapid surface charge transfer. Moreover the CV results reveal that ECL response can also be tuned by carefully selecting the precursors [151]. As the value of current increases, $SO_4^{\circ-}$ and SO_4^{2-} radicals are generated by the breakdown of coreactant $S_2O_8^-$, leading to the rise in excited states. At the cathode, EM field increases due to accumulation of free electrons resulting from the SPR phenomena where these electrons combine with the excitons of MQDs and improve ECL generation [152]. These MQDs were further used to create a functional sensor to detect miRNA-26a which is important for the diagnosis of triple negative breast cancer. The sensitivity of this nanomaterial-based device is higher than available microarray and RTPCR techniques, since it can detect target miRNA concentration up to 5 fM. These studies are evidence that MXenes have a huge market in the biomedical world as well if they are synthesized to be biocompatible. These composites can be used intrinsically for bio-imaging, sensing, tumor cell diagnosis as well as treatment.

4.3. Catalysis and allied applications

In the era of rigorous industrialisation, the discharge of industrial effluents and other harmful wet chemicals poses a serious hazard to the environment. Such industrial wastewaters are generally highly toxic and non-degradable in nature [153–158]. A study by Chen et al. centres around catalytic reduction of 4-nitro [1]phenol (4-NP), 2-nitrophenol (2-NP), methylene blue (MB) and methyl orange (MO) by palladium nanoparticle (np) loaded on polydopamine (PDA) decorated MXene sheets [159]. During the course of the study, catalytic performance was measured at specific absorption wavelengths with change in pollutant concentration. Also, sodium borohydride was added for activating the reduction process. The highly dense and uniformly dispersed Pd possess abundant activation sites that aid in the electron transfer rate. These anchor on the surface due to the reduction of PDA and Ti_3C_2, masking some activation sites on Ti_3C_2 while more PDA active sites evolve. Through catalytic reduction efficiency analysis, it can be said that PDA aid in uniform loading as well as accelerate 2-NP adsorption at the catalytic surface, promoting interaction between active sites and 2-NP (Fig. 8).

Another aspect of this study is the reusability of MXene sheets as the recycling ability of a catalyst holds a vital index when considering its overall efficiency. This argument was supported by repetitive catalytic testing for all the four pollutants evaluating catalytic capacity for each cycle [160]. It exhibits 92% efficacy after 10 cycles with a minimal palladium leaching of not more than 1.2% for one cycle. In a similar work, Keding Li et al. explored the effect of cobaltosic oxide loaded MXene nanocomposite (Co-MX) for thermal decomposition of ammonium perchlorate (NH_4ClO_4) [161]. Among different concentrations of Co-MX complex, 20 wt% could substantially lower the high thermal decomposition (HTD) temperature by 118.9 °C. This significant decrease is due to large specific surface area of Co-MX complex facilitating better contact between NH_4ClO_4 and Co-NPs. For promoting the decomposition of NH_4ClO_4, catalyst can aid in lowering the activation energy and increase the reaction rate [162].

Due to the adsorption effect at the surface of NH_4ClO_4 there would be incomplete reaction between $HClO_4$ and NH_3 which would result in a stacked structure between $HClO_4$ and NH_3 while impeding the decomposition of NH_4ClO_4. But, with addition of Co-MX; the LTD stage of NH_4ClO_4 vanished suggesting improvement in the reactivity of $HClO_4$ with NH_3. These studies offer green synthetic approach by tailoring terminating groups at the surface rendering them as a reduction active site with electron transport.

Moving forth, leveraging the mechanical, surficial functionalities and electro-thermal conductivity, Wonsik Eom et al. developed an additive synthetic route to fashion pure MXene fibres via wet spinning [42]. The obtained MXene fibres are employed for transmitting electronic signals to earphones and as electrical wires in LEDs replacing commercially used wires featuring applicability in miniaturized portable and wearable electronics. The dispersion of $Ti_3C_2T_x$ MXene sheets averaging 5.11 μm^2 exhibits extremely stable colloidal features in a lyotropic liquid crystalline phase. With wet spinning strategy, the research group was able to produce highly flexible and continuous MXene fibres (1 m in length) showcasing very high conductivity (7713 S/cm) as compared to 72.3 and 290 S/cm of MXene and graphene hybrid fibers respectively) [163,164]. During the fabrication, an increase in negative surface charge was observed which can be due to the presence of ionizing surface terminations, pointing towards strong electrostatic repulsion among the adjacent sheets. With many studies revolving around dispersion of MXene fibres, it is now an established fact that in order to obtain a continuous fibre assembly, a very high degree of gelation and exfoliation is required. For this reason. ammonium ions were introduced during the coagulation process to yield gel fibers. A lamellar architecture with compactly packed nanosheets and rough morphology on the edges was observed. The study provides an insight to explore nanoscale potential of MXenes at a macro scale with a footprint in scalable and flexible wearable electronics.

5. Discussion

The growing research in MXenes will transform the next 10 years in sectors like microelectronics, robotics, biomedical, aerospace etc. Green

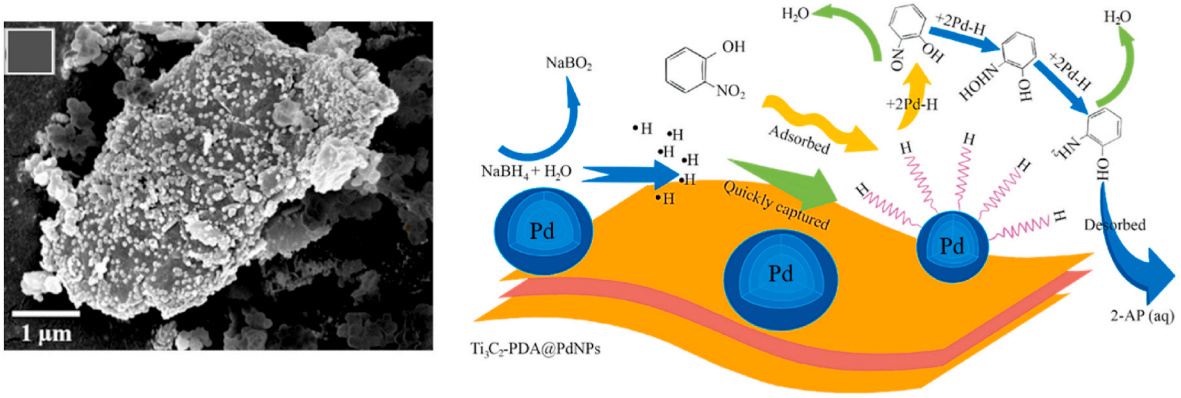

Fig. 8. SEM image showing MXene decorated with Pd nanoparticles, and on the right the infographic describes the inherent catalytic mechanism. Adapted with permission from Ref. [159]. Copyright 2021, Elsevier.

synthesis of structures with nanoribbons or nanotubes should be looked upon to observe the impact of one-dimensional ensembles commercially. The main idea behind exploring green MXenes is to take a conscious step in contributing towards the goal of sustainable future. In this study the defining parameters for green MXenes were focused on precursors, energy consumption and green solvents! However there are other factors as well that make a material sustainable for example, overall cost, LCA parameters (cradle to grave analysis – type of chemicals, supply chains, recyclability and degradation). Nevertheless, to broaden the scope of this study, an attempt is made to create a roadmap of globally significant factors that govern material industry (Fig. 9). We establish that MXene costs can be reduced from $1500 per ton for conventionally prepared MXenes to about $1 (device cost) for green MXenes developed using mass nanofabrication with the help of SAW device (acoustic exfoliation). Green MXenes can thus increase the accessibility and affordability of high efficiency energy rich material.

6. Conclusion and future perspective

2-dimensional materials have the potential to help address the global energy demand. Herein, we identified MXenes and MXene derivatives and gathered interpretations of their mechanical and electrical characteristics. It was evident in the materials community that a sustainable, green synthetic approach along with the underlying optimization of physical and chemical properties are key contributors for real world application of any material; MXenes can be contemplated as an enabling technology in the field of energy storage and conversion. The following conclusions can be drawn from this article, that might interest the reader in brainstorming possible solutions for efficient devices. Traditionally, MXene synthesis was realized with direct HF etching or employing acid containing F ions. HF, known to be highly toxic in nature, has severe environmental implications and eventually hinders the applicability of MXene in fields of biomedical and energy storage applications. This presents a major research essentiality and possibility to look for greener substitutes. Among the many green synthetic routes suggested for curbing intermolecular oxidation, addition of bio oxidants and deep eutectic solvents for preparing large-sized MXene complexes prolong the structural and functional life of MXene molecules. Intercalation of high molecular weight ionic liquids has shown drastic reduction in oxidation rate and is regarded as a greener substitute. An exhaustive understanding of MXene surface morphology and electroactive mechanisms is desired. A continuous exploration of etchants and solvents that not only stabilize MXene suspensions but enhance surface functionalization is needed. Defects are regarded as dipole active sites that induce deflection in the geometric centre of passing electrons, in turn delivering dipole and interface polarization. These can be artificially introduced in MXene sheets via external bias, electric/magnetic field, chemical etching or in situ degradation of certain ionic species. In ternary heterocomposites, the increase in number of interfaces encourages easy electron hopping by limiting the phase charge accumulation and impedance mismatch. MXene composites are selective catalysts and their selectivity can be experimentally quantified by maintaining an optimal overpotential. Other quantitative tools like Faraday efficiency, production rate, Gibbs free energy and apparent quantum yield are also considered for estimating the efficiency of MXene catalysts. Green-MXenes can be contemplated as an enabling technology in the field of energy storage and conversion for its properties like high specific capacitance, pseudocapacitive charge storage mechanism and stability. Additionally, nature derived MXenes integrated in bio-sensing platforms are promising solutions for tumor diagnosis and treatment due to their non-toxicity, high surface area and enhanced photothermal conversion ability. Given the combination of properties like large surface area, excellent hydrophilicity, high conductivity and rich laboratory-tailoring ability; MXenes hold great potential in both electro-chemical and heterogeneous catalytic reactions. Moreover, in order to expand their catalytic applicability, interplay of metal elements with surface termination modalities needs further investigation. To bridge the gap between existing MXene configurations and desired properties, computational studies provide a foresight for understanding solvent–MXene; intercalant-MXene interactions, reaction thermodynamics and bandgap projections to optimize the molecular structure.

This understanding of nature sensitive MXenes can be further refined by integrating AI tools to assess chemical life and end products. The criteria of green MXenes can be further extended to those that can be

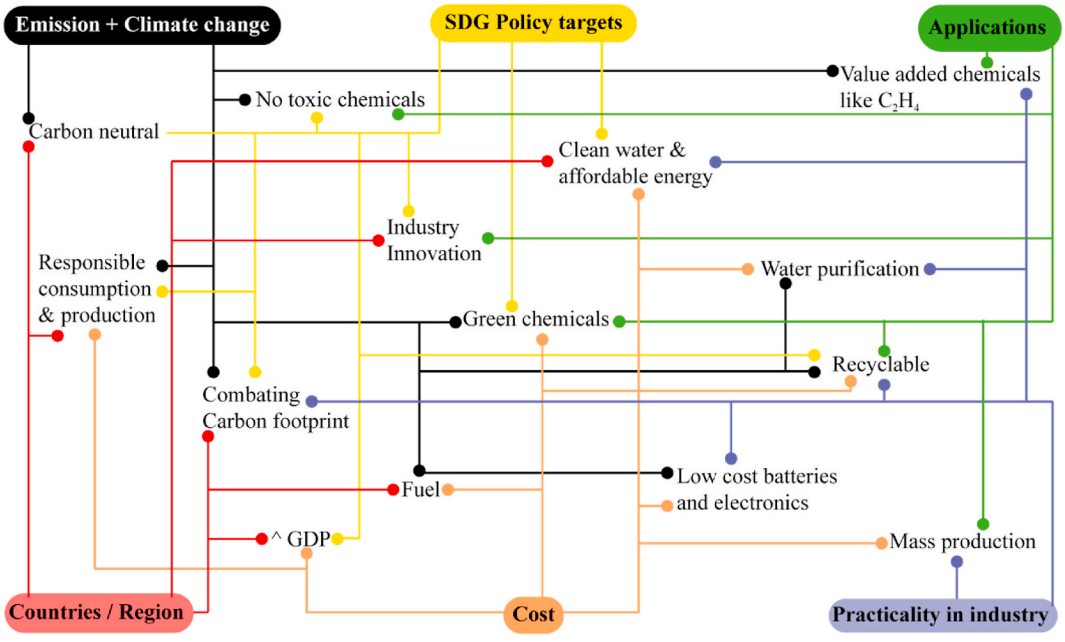

Fig. 9. Infographic wireframe, mapping the impact of green MXenes on global platform. Sustainable development goals (SDG) like clean water and affordable energy can be visualized with the low cost, climate sensitive MXene systems, similarly factors like accessible fuel, recyclable material or scalable synthesis influence the economic growth of any country. This wireframe can be followed to analyse the interdependency of fundamental factors including zero toxic waste, ease of adaptability and stability of 2D MXenes.

mass produced, form composites with other green materials like biochar, cellulose etc; undergo recycling and are cost effective. This review establishes as the primary account of the potential of MXenes to transform energy industry keeping in check with the sustainable development goals. MXenes can therefore be the most dependable material to achieve carbon-neutrality, safe water, pollution reduction and energy independent targets not only in large economies but also in developing countries.

Declaration of competing interest

The authors declare that they have no known competing financial interests or personal relationships that could have appeared to influence the work reported in this paper.

Data availability

No data was used for the research described in the article.

Acknowledgement

The authors would like to thank Dr CP Ramanarayanan, Vice-Chancellor, Defence Institute of Advanced Technology (DU), Pune for the support. Shatakshi Saxena would particularly like to thank Dr. K.V. R. Rao, Director, Centre for Converging Technologies (CCT), Jaipur and Dr. V.K Saxena, additional director, CCT, Jaipur for their constant guidance and mentorship. I would also return the regard by thanking Mr Prakash Gore and Ms Niranjana Jaya Prakash, PhD scholars at DIAT for the technical help due the course.

References

[1] Butler SZ, Hollen SM, Cao L, Cui Y, Gupta JA, Gutiérrez HR, et al. Progress, challenges, and opportunities in two-dimensional materials beyond graphene. ACS Nano 2013;7:2898–926. https://doi.org/10.1021/nn400280c.
[2] Tiwari S, Purabgola A, Kandasubramanian B. Functionalised graphene as flexible electrodes for polymer photovoltaics. J Alloys Compd 2020;825:153954. https://doi.org/10.1016/j.jallcom.2020.153954.
[3] Prajapati DG, Kandasubramanian B. Biodegradable polymeric solid framework-based organic phase-change materials for thermal energy storage. Ind Eng Chem Res 2019. https://doi.org/10.1021/acs.iecr.9b01693.
[4] Ding M, Li S, Guo L, Jing L, Gao SP, Yang H, et al. Metal ion-induced assembly of MXene aerogels via biomimetic microtextures for electromagnetic interference shielding, capacitive deionization, and microsupercapacitors. Adv Energy Mater 2021;11:2101494. https://doi.org/10.1002/aenm.202101494.
[5] Jiang H, Li J, Li Y, Liang M, Huang F, Wang Y, et al. Gill inspired hierarchical wrinkles of reduced graphene oxide encapsulated carbon nanotubes with significantly boosted supercapacitor performance. Ceram Int 2021;47:26712–9. https://doi.org/10.1016/j.ceramint.2021.06.078.
[6] Magisetty R, Kumar P, Kumar V, Shukla A, Kandasubramanian B, Shunmugam R. NiFe2O4/Poly(1,6-heptadiyne) nanocomposite energy-storage device for electrical and electronic applications. ACS Omega 2018;3:15256–66. https://doi.org/10.1021/acsomega.8b02306.
[7] Suresh Khurd A, Kandasubramanian B. A systematic review of cellulosic material for green electronics devices. Carbohydr Polym Technol Appl 2022;4:100234. https://doi.org/10.1016/j.carpta.2022.100234.
[8] Ariyamparambil VJ, Kandasubramanian B. A mini-review on the recent advancement of electrospun MOF-derived nanofibers for energy storage. Chem Eng J Adv 2022;11:100355. https://doi.org/10.1016/j.ceja.2022.100355.
[9] Das S, Robinson JA, Dubey M, Terrones H, Terrones M. Beyond graphene: progress in novel two-dimensional materials and van der Waals solids. Annu Rev Mater Res 2015;45:1–27. https://doi.org/10.1146/annurev-matsci-070214-021034.
[10] Naguib M, Barsoum MW, Gogotsi Y. Ten years of progress in the synthesis and development of MXenes. Adv Mater 2021;33:2103393. https://doi.org/10.1002/adma.202103393.
[11] Zhan X, Si C, Zhou J, Sun Z. MXene and MXene-based composites: synthesis, properties and environment-related applications. Nanoscale Horizons 2020;5:235–58. https://doi.org/10.1039/C9NH00571D.
[12] Montazeri K, Currie M, Verger L, Dianat P, Barsoum MW, Nabet B. Beyond gold: spin-coated Ti 3 C 2 -based MXene photodetectors. Adv Mater 2019;31:1903271. https://doi.org/10.1002/adma.201903271.
[13] Huang S, Mutyala KC, Sumant AV, Mochalin VN. Achieving superlubricity with 2D transition metal carbides (MXenes) and MXene/graphene coatings. Mater Today Adv 2021;9:100133. https://doi.org/10.1016/j.mtadv.2021.100133.
[14] Zhao Q, Zhu Q, Miao J, Zhang P, Wan P, He L, et al. Flexible 3D porous MXene foam for high-performance lithium-ion batteries. Small 2019;15:1–9. https://doi.org/10.1002/smll.201904293.
[15] Abdolhosseinzadeh S, Schneider R, Verma A, Heier J, Nüesch F, Zhang C. Turning trash into treasure: additive free MXene sediment inks for screen-printed micro-supercapacitors. Adv Mater 2020;32:2000716. https://doi.org/10.1002/adma.202000716.
[16] Soleymaniha M, Shahbazi MA, Rafieerad AR, Maleki A, Amiri A. Promoting role of MXene nanosheets in biomedical sciences: therapeutic and biosensing innovations. Adv Healthc Mater 2019;8:1801137. https://doi.org/10.1002/adhm.201801137.
[17] George SM, Kandasubramanian B. Advancements in MXene-Polymer composites for various biomedical applications. Ceram Int 2020;46:8522–35. https://doi.org/10.1016/j.ceramint.2019.12.257.
[18] Dixit F, Zimmermann K, Dutta R, Prakash NJ, Barbeau B, Mohseni M, et al. Application of MXenes for water treatment and energy-efficient desalination: a review. J Hazard Mater 2022;423:127050. https://doi.org/10.1016/j.jhazmat.2021.127050.
[19] Dixit F, Munoz G, Mirzaei M, Barbeau B, Liu J, Duy SV, et al. Removal of zwitterionic PFAS by MXenes: comparisons with anionic, nonionic, and PFAS-specific resins. Environ Sci Technol 2021;56:6212–22. https://doi.org/10.1021/acs.est.1c03780.
[20] Qin L, Jiang J, Tao Q, Wang C, Persson I, Fahlman M, et al. A flexible semitransparent photovoltaic supercapacitor based on water-processed MXene electrodes. J Mater Chem 2020;8:5467–75. https://doi.org/10.1039/D0TA00687D.
[21] Qu D, Jian Y, Guo L, Su C, Tang N, Zhang X, et al. An organic solvent-assisted intercalation and collection (OAIC) for Ti3C2Tx MXene with controllable sizes and improved yield. Nano-Micro Lett 2021;13:188. https://doi.org/10.1007/s40820-021-00705-4.
[22] Jaya Prakash N, Kandasubramanian B. Nanocomposites of MXene for industrial applications. J Alloys Compd 2021;862:158547. https://doi.org/10.1016/j.jallcom.2020.158547.
[23] Jaya Prakash N, Kandasubramanian B. Industrial applications of MXene nanocomposites. Nanoparticle-Based Polym. Compos.. Elsevier; 2022. p. 481–503. https://doi.org/10.1016/B978-0-12-824272-8.00010-5.
[24] He P, Cao M-S, Cai Y-Z, Shu J-C, Cao W-Q, Yuan J. Self-assembling flexible 2D carbide MXene film with tunable integrated electron migration and group relaxation toward energy storage and green EMI shielding. Carbon N Y 2020;157:80–9. https://doi.org/10.1016/j.carbon.2019.10.009.
[25] Zhang K, Sun J, Song J, Gao C, Wang Z, Song C, et al. Self-healing Ti3C2MXene/PDMS supramolecular elastomers based on small biomolecules modification for wearable sensors. ACS Appl Mater Interfaces 2020;12:45306–14. https://doi.org/10.1021/acsami.0c13653.
[26] Liang G, Li X, Wang Y, Yang S, Huang Z, Yang Q, et al. Building durable aqueous K-ion capacitors based on MXene family. Nano Res Energy 2022;1:e9120002. https://doi.org/10.26599/NRE.2022.9120002.
[27] Zhang YZ, Wang Y, Jiang Q, El-Demellawi JK, Kim H, Alshareef HN. MXene printing and patterned coating for device applications. Adv Mater 2020;32:1908486. https://doi.org/10.1002/adma.201908486.
[28] Sarycheva A, Polemi A, Liu Y, Dandekar K, Anasori B, Gogotsi Y. 2D titanium carbide (MXene) for wireless communication. Sci Adv 2018;4. https://doi.org/10.1126/sciadv.aau0920.
[29] Riazi H, Nemani SK, Grady MC, Anasori B, Soroush M. Ti 3 C 2 MXene–polymer nanocomposites and their applications. J Mater Chem 2021;9:8051–98. https://doi.org/10.1039/D0TA08023C.
[30] Yang W, Byun JJ, Yang J, Moissinac FP, Peng Y, Tontini G, et al. Freeze-assisted tape casting of vertically aligned MXene films for high rate performance supercapacitors. Energy Environ Mater 2020;3:380–8. https://doi.org/10.1002/eem2.12106.
[31] Jiang X, Li W, Hai T, Yue R, Chen Z, Lao C, et al. Inkjet-printed MXene micro-scale devices for integrated broadband ultrafast photonics. Npj 2D Mater Appl 2019;3:34. https://doi.org/10.1038/s41699-019-0117-3.
[32] Luo L, Huang Y, Cheng K, Alhassan A, Alqahtani M, Tang L, et al. MXene-GaN van der Waals metal-semiconductor junctions for high performance multiple quantum well photodetectors. Light Sci Appl 2021;10:177. https://doi.org/10.1038/s41377-021-00619-1.
[33] Huang Y-L, Bian S-W. Vacuum-filtration assisted layer-by-layer strategy to design MXene/carbon nanotube@MnO 2 all-in-one supercapacitors. J Mater Chem 2021;9:21347–56. https://doi.org/10.1039/D1TA06089A.
[34] Wan Y-J, Li X-M, Zhu P-L, Sun R, Wong C-P, Liao W-H. Lightweight, flexible MXene/polymer film with simultaneously excellent mechanical property and high-performance electromagnetic interference shielding. Compos Part A Appl Sci Manuf 2020;130:105764. https://doi.org/10.1016/j.compositesa.2020.105764.
[35] Habib T, Patil N, Zhao X, Prehn E, Anas M, Lutkenhaus JL, et al. Heating of Ti3C2Tx MXene/polymer composites in response to Radio Frequency fields. Sci Rep 2019;9:16489. https://doi.org/10.1038/s41598-019-52972-2.
[36] Ren A, Zou J, Lai H, Huang Y, Yuan L, Xu H, et al. Direct laser-patterned MXene–perovskite image sensor arrays for visible-near infrared photodetection. Mater Horiz 2020;7:1901–11. https://doi.org/10.1039/D0MH00537A.
[37] Abdolhosseinzadeh S, Heier J, Zhang C. Printing and coating MXenes for electrochemical energy storage devices. JPhys Energy 2020;2:031004. https://doi.org/10.1088/2515-7655/aba47d.
[38] Sreenilayam SP, Ul Ahad I, Nicolosi V, Brabazon D. MXene materials based printed flexible devices for healthcare, biomedical and energy storage

applications. Mater Today 2021;43:99–131. https://doi.org/10.1016/j.mattod.2020.10.025.
[39] Xu S, Dall'Agnese Y, Wei G, Zhang C, Gogotsi Y, Han W. Screen-printable microscale hybrid device based on MXene and layered double hydroxide electrodes for powering force sensors. Nano Energy 2018;50:479–88. https://doi.org/10.1016/j.nanoen.2018.05.064.
[40] Yang W, Yang J, Byun JJ, Moissinac FP, Xu J, Haigh SJ, et al. 3D printing of freestanding MXene architectures for current-collector-free supercapacitors. Adv Mater 2019;31:1902725. https://doi.org/10.1002/adma.201902725.
[41] Redondo E, Pumera M. MXene-functionalised 3D-printed electrodes for electrochemical capacitors. Electrochem Commun 2021;124:106920. https://doi.org/10.1016/j.elecom.2021.106920.
[42] Eom W, Shin H, Ambade RB, Lee SH, Lee KH, Kang DJ, et al. Large-scale wet-spinning of highly electroconductive MXene fibers. Nat Commun 2020;11:2825. https://doi.org/10.1038/s41467-020-16671-1.
[43] Levitt AS, Alhabeb M, Hatter CB, Sarycheva A, Dion G, Gogotsi Y. Electrospun MXene/carbon nanofibers as supercapacitor electrodes. J Mater Chem 2019;7:269–77. https://doi.org/10.1039/C8TA09810G.
[44] Jimmy J, Kandasubramanian B. Mxene functionalized polymer composites: synthesis and applications. Eur Polym J 2020;122:109367. https://doi.org/10.1016/j.eurpolymj.2019.109367.
[45] Yu S, Tang H, Zhang D, Wang S, Qiu M, Song G, et al. MXenes as emerging nanomaterials in water purification and environmental remediation. Sci Total Environ 2022;811:152280. https://doi.org/10.1016/j.scitotenv.2021.152280.
[46] Ghazaly A El, Zheng W, Halim J, Tseng EN, Persson PO, Ahmed B, et al. Enhanced supercapacitive performance of Mo1.33C MXene based asymmetric supercapacitors in lithium chloride electrolyte. Energy Storage Mater 2021;41:203–8. https://doi.org/10.1016/j.ensm.2021.05.006.
[47] Cao W-T, Chen F-F, Zhu Y-J, Zhang Y-G, Jiang Y-Y, Ma M-G, et al. Binary strengthening and toughening of MXene/cellulose nanofiber composite paper with nacre-inspired structure and superior electromagnetic interference shielding properties. ACS Nano 2018;12:4583–93. https://doi.org/10.1021/acsnano.8b00997.
[48] Hart JL, Hantanasirisakul K, Lang AC, Anasori B, Pinto D, Pivak Y, et al. Control of MXenes' electronic properties through termination and intercalation. Nat Commun 2019;10:1–10. https://doi.org/10.1038/s41467-018-08169-8.
[49] Lotfi R, Naguib M, Yilmaz DE, Nanda J, van Duin ACT. A comparative study on the oxidation of two-dimensional Ti 3 C 2 MXene structures in different environments. J Mater Chem 2018;6:12733–43. https://doi.org/10.1039/C8TA01468J.
[50] Zhao X, Holta DE, Tan Z, Oh J-H, Echols IJ, Anas M, et al. Annealed Ti 3 C 2 T z MXene films for oxidation-resistant functional coatings. ACS Appl Nano Mater 2020;3:10578–85. https://doi.org/10.1021/acsanm.0c02473.
[51] Zhang CJ, Pinilla S, McEvoy N, Cullen CP, Anasori B, Long E, et al. Oxidation stability of colloidal two-dimensional titanium carbides (MXenes). Chem Mater 2017;29:4848–56. https://doi.org/10.1021/acs.chemmater.7b00745.
[52] Nasrallah GK, Al-Asmakh M, Rasool K, Mahmoud KA. Ecotoxicological assessment of Ti 3 C 2 T x (MXene) using a zebrafish embryo model. Environ Sci Nano 2018;5:1002–11. https://doi.org/10.1039/C7EN01239J.
[53] Shuck CE, Ventura-Martinez K, Goad A, Uzun S, Shekhirev M, Gogotsi Y. Safe synthesis of MAX and MXene: guidelines to reduce risk during synthesis. ACS Chem Heal Saf 2021;28:326–38. https://doi.org/10.1021/acs.chas.1c00051.
[54] Alhabeb M, Maleski K, Anasori B, Lelyukh P, Clark L, Sin S, et al. Guidelines for synthesis and processing of two-dimensional titanium carbide (Ti 3 C 2 T x MXene). Chem Mater 2017;29:7633–44. https://doi.org/10.1021/acs.chemmater.7b02847.
[55] Lakhe P, Prehn EM, Habib T, Lutkenhaus JL, Radovic M, Mannan MS, et al. Process safety analysis for Ti 3 C 2 T x MXene synthesis and processing. Ind Eng Chem Res 2019;58:1570–9. https://doi.org/10.1021/acs.iecr.8b05416.
[56] Zhang Y, Liu H, Gao F, Tan X, Cai Y, Hu B, et al. Application of MOFs and COFs for photocatalysis in CO2 reduction, H2 generation, and environmental treatment. Energy 2022;4:100078. https://doi.org/10.1016/j.enchem.2022.100078.
[57] Lu Y, Cai Y, Zhang S, Zhuang L, Hu B, Wang S, et al. Application of biochar-based photocatalysts for adsorption-(photo)degradation/reduction of environmental contaminants: mechanism, challenges and perspective. Biochar 2022;4:45. https://doi.org/10.1007/s42773-022-00173-y.
[58] Han M, Shuck CE, Rakhmanov R, Parchment D, Anasori B, Koo CM, et al. Beyond Ti 3 C 2 T x : MXenes for electromagnetic interference shielding. ACS Nano 2020;14:5008–16. https://doi.org/10.1021/acsnano.0c01312.
[59] Gogotsi Y, Anasori B. The rise of MXenes. ACS Nano 2019;13:8491–4. https://doi.org/10.1021/acsnano.9b06394.
[60] Shpigel N, Chakraborty A, Malchik F, Bergman G, Nimkar A, Gavriel B, et al. Can anions Be inserted into MXene? J Am Chem Soc 2021;143:12552–9. https://doi.org/10.1021/jacs.1c03840.
[61] Hemanth NR, Kandasubramanian B. Recent advances in 2D MXenes for enhanced cation intercalation in energy harvesting Applications: a review. Chem Eng J 2020;392:123678. https://doi.org/10.1016/j.cej.2019.123678.
[62] Nguyen VH, Tabassian R, Oh S, Nam S, Mahato M, Thangasamy P, et al. Stimuli-responsive MXene-based actuators. Adv Funct Mater 2020;30:1–27. https://doi.org/10.1002/adfm.201909504.
[63] Han M, Shuck CE, Rakhmanov R, Parchment D, Anasori B, Koo CM, et al. Beyond Ti3C2Tx: MXenes for electromagnetic interference shielding. ACS Nano 2020;14:5008–16. https://doi.org/10.1021/acsnano.0c01312.
[64] Liu X, Verma G, Chen Z, Hu B, Huang Q, Yang H, et al. Metal-organic framework nanocrystal-derived hollow porous materials: synthetic strategies and emerging applications. Innovation 2022;3:100281. https://doi.org/10.1016/j.xinn.2022.100281.
[65] Liu Z, Xu Z, Xu L, Buyong F, Chay TC, Li Z, et al. Modified biochar: synthesis and mechanism for removal of environmental heavy metals. Carbon Res 2022;1:8. https://doi.org/10.1007/s44246-022-00007-3.
[66] Dixit F, Zimmermann K, Alamoudi M, Abkar L, Barbeau B, Mohseni M, et al. Application of MXenes for air purification, gas separation and storage: a review. Renew Sustain Energy Rev 2022;164:112527. https://doi.org/10.1016/j.rser.2022.112527.
[67] Khazaei M, Arai M, Sasaki T, Chung CY, Venkataramanan NS, Estili M, et al. Novel electronic and magnetic properties of two-dimensional transition metal carbides and nitrides. Adv Funct Mater 2013;23:2185–92. https://doi.org/10.1002/adfm.201202502.
[68] Enyashin AN, Ivanovskii AL. Two-dimensional titanium carbonitrides and their hydroxylated derivatives: structural, electronic properties and stability of MXenes Ti3C 2-xNx(OH)2 from DFTB calculations. J Solid State Chem 2013;207:42–8. https://doi.org/10.1016/j.jssc.2013.09.010.
[69] Tahir M, Ali Khan A, Tasleem S, Mansoor R, Fan WK. Titanium carbide (Ti 3 C 2) MXene as a promising Co-catalyst for photocatalytic CO 2 conversion to energy-efficient fuels: a review. Energy Fuels 2021;35:10374–404. https://doi.org/10.1021/acs.energyfuels.1c00958.
[70] Zhao MQ, Torelli M, Ren CE, Ghidiu M, Ling Z, Anasori B, et al. 2D titanium carbide and transition metal oxides hybrid electrodes for Li-ion storage. Nano Energy 2016;30:603–13. https://doi.org/10.1016/j.nanoen.2016.10.062.
[71] Nemani SK, Zhang B, Wyatt BC, Hood ZD, Manna S, Khaledialidusti R, et al. High-entropy 2D carbide MXenes: TiVNbMoC 3 and TiVCrMoC 3. ACS Nano 2021;15:12815–25. https://doi.org/10.1021/acsnano.1c02775.
[72] Deysher G, Shuck CE, Hantanasirisakul K, Frey NC, Foucher AC, Maleski K, et al. Synthesis of Mo 4 VAlC 4 MAX phase and two-dimensional Mo 4 VC 4 MXene with five atomic layers of transition metals. ACS Nano 2020;14:204–17. https://doi.org/10.1021/acsnano.9b07708.
[73] Chertopalov S, Mochalin VN. Environment-sensitive photoresponse of spontaneously partially oxidized Ti3C2 MXene thin films. ACS Nano 2018;12:6109–16. https://doi.org/10.1021/acsnano.8b02379.
[74] Ghazaly A El, Ahmed H, Rezk AR, Halim J, Persson POÅ, Yeo LY, et al. Ultrafast, one-step, salt-solution-based acoustic synthesis of Ti 3 C 2 MXene. ACS Nano 2021;15:4287–93. https://doi.org/10.1021/acsnano.0c07242.
[75] Sarycheva A, Gogotsi Y. Raman spectroscopy analysis of the structure and surface chemistry of Ti3C2T xMXene. Chem Mater 2020;32:3480–8. https://doi.org/10.1021/acs.chemmater.0c00359.
[76] Cheng Y, Ma Y, Li L, Zhu M, Yue Y, Liu W, et al. Bioinspired microspines for a high-performance spray Ti3C2Tx MXene-based piezoresistive sensor. ACS Nano 2020;14:2145–55. https://doi.org/10.1021/acsnano.9b08952.
[77] Ma W, Cai W, Chen W, Liu P, Wang J, Liu Z. A novel structural design of shielding capsule to prepare high-performance and self-healing MXene-based sponge for ultra-efficient electromagnetic interference shielding. Chem Eng J 2021;426:130729. https://doi.org/10.1016/j.cej.2021.130729.
[78] Yang K, Luo M, Zhang D, Liu C, Li Z, Wang L, et al. Ti3C2Tx/carbon nanotube/porous carbon film for flexible supercapacitor. Chem Eng J 2022;427:132002. https://doi.org/10.1016/j.cej.2021.132002.
[79] Yao Y, Lan L, Liu X, Ying Y, Ping J. Spontaneous growth and regulation of noble metal nanoparticles on flexible biomimetic MXene paper for bioelectronics. Biosens Bioelectron 2020;148:111799. https://doi.org/10.1016/j.bios.2019.111799.
[80] Huang H, Song Y, Li N, Chen D, Xu Q, Li H, et al. One-step in-situ preparation of N-doped TiO2@C derived from Ti3C2 MXene for enhanced visible-light driven photodegradation. Appl Catal B Environ 2019;251:154–61. https://doi.org/10.1016/j.apcatb.2019.03.066.
[81] Wang J, Liu Y, Cheng Z, Xie Z, Yin L, Wang W, et al. Highly conductive MXene film actuator based on moisture gradients. Angew Chem Int Ed 2020;59:14029–33. https://doi.org/10.1002/anie.202003737.
[82] Yu H, Wang Y, Jing Y, Ma J, Du C, Yan Q. Surface modified MXene-based nanocomposites for electrochemical energy conversion and storage. Small 2019;15:1901503. https://doi.org/10.1002/smll.201901503.
[83] Ma W, Cai W, Chen W, Liu P, Wang J, Liu Z. Microwave-induced segregated composite network with MXene as interfacial solder for ultra-efficient electromagnetic interference shielding and anti-dripping. Chem Eng J 2021;425:131699. https://doi.org/10.1016/j.cej.2021.131699.
[84] Li X, Li M, Li X, Fan X, Zhi C. Low infrared emissivity and strong stealth of Ti-based MXenes. Research 2022;2022:1–7. https://doi.org/10.34133/2022/9892628.
[85] Han M, Shuck CE, Singh A, Yang Y, Foucher AC, Goad A, et al. Efficient microwave absorption with Vn+1CnT MXenes. Cell Reports Phys Sci 2022;3:101073. https://doi.org/10.1016/j.xcrp.2022.101073.
[86] Lipatov A, Alhabeb M, Lukatskaya MR, Boson A, Gogotsi Y, Sinitskii A. Effect of synthesis on quality, electronic properties and environmental stability of individual monolayer Ti3C2 MXene flakes. Adv Electron Mater 2016;2:1600255. https://doi.org/10.1002/aelm.201600255.
[87] Naguib M, Mashtalir O, Carle J, Presser V, Lu J, Hultman L, et al. Two-dimensional transition metal carbides. ACS Nano 2012;6:1322–31. https://doi.org/10.1021/nn204153h.
[88] Khazaei M, Arai M, Sasaki T, Ranjbar A, Liang Y, Yunoki S. OH-terminated two-dimensional transition metal carbides and nitrides as ultralow work function materials. Phys Rev B Condens Matter 2015;92:075411. https://doi.org/10.1103/PhysRevB.92.075411.

[89] Xia F, Lao J, Yu R, Sang X, Luo J, Li Y, et al. Ambient oxidation of Ti 3 C 2 MXene initialized by atomic defects. Nanoscale 2019;11:23330–7. https://doi.org/10.1039/C9NR07236E.
[90] Fayyaz A, Saravanakumar K, Talukdar K, Kim Y, Yoon Y, Park CM. Catalytic oxidation of naproxen in cobalt spinel ferrite decorated Ti3C2Tx MXene activated persulfate system: mechanisms and pathways. Chem Eng J 2021;407:127842. https://doi.org/10.1016/j.cej.2020.127842.
[91] Yin G, Wang Y, Wang W, Yu D. Multilayer structured PANI/MXene/CF fabric for electromagnetic interference shielding constructed by layer-by-layer strategy. Colloids Surfaces A Physicochem Eng Asp 2020;601:125047. https://doi.org/10.1016/j.colsurfa.2020.125047.
[92] Xia Y, Mathis TS, Zhao MQ, Anasori B, Dang A, Zhou Z, et al. Thickness-independent capacitance of vertically aligned liquid-crystalline MXenes. Nature 2018;557:409–12. https://doi.org/10.1038/s41586-018-0109-z.
[93] Ghidiu M, Lukatskaya MR, Zhao M-Q, Gogotsi Y, Barsoum MW. Conductive two-dimensional titanium carbide 'clay' with high volumetric capacitance. Nature 2014;516:78–81. https://doi.org/10.1038/nature13970.
[94] Lukatskaya MR, Mashtalir O, Ren CE, Dall'Agnese Y, Rozier P, Taberna PL, et al. Cation intercalation and high volumetric capacitance of two-dimensional titanium carbide. Science 2013;341(80):1502–5. https://doi.org/10.1126/science.1241488.
[95] Zheng H, Wang Y, Niu B, Ge R, Lei Y, Yan L, et al. Controlling the defect density of perovskite films by MXene/SnO2Hybrid electron transport layers for efficient and stable photovoltaics. J Phys Chem C 2021;125:15210–22. https://doi.org/10.1021/acs.jpcc.1c04361.
[96] Wang Y, Lubbers T, Xia R, Zhang Y-Z, Mehrali M, Huijben M, et al. Printable two-dimensional V 2 O 5/MXene heterostructure cathode for lithium-ion battery. J Electrochem Soc 2021;168:020507. https://doi.org/10.1149/1945-7111/abdef2.
[97] Rajavel K, Yu X, Zhu P, Hu Y, Sun R, Wong C. Exfoliation and defect control of two-dimensional few-layer MXene Ti3C2T xfor electromagnetic interference shielding coatings. ACS Appl Mater Interfaces 2020;12:49737–47. https://doi.org/10.1021/acsami.0c12835.
[98] Wang S, Shao H-Q, Liu Y, Tang C-Y, Zhao X, Ke K, et al. Boosting piezoelectric response of PVDF-TrFE via MXene for self-powered linear pressure sensor. Compos Sci Technol 2021;202:108600. https://doi.org/10.1016/j.compscitech.2020.108600.
[99] Library PY, Hom H, Kong H. Preparation of graphene and graphene- analogue two-dimensional nanomaterials and their applications in electronics Ph . D The Hong Kong Polytechnic University [n.d].
[100] Li X, Wen C, Yuan M, Sun Z, Wei Y, Ma L, et al. Nickel oxide nanoparticles decorated highly conductive Ti3C2 MXene as cathode catalyst for rechargeable Li–O2 battery. J Alloys Compd 2020;824:153803. https://doi.org/10.1016/j.jallcom.2020.153803.
[101] Zhang H, Li Z, Hou Z, Mei H, Feng Y, Xu B, et al. Self-assembly of MOF on MXene nanosheets and in-situ conversion into superior nickel phosphates/MXene battery-type electrode. Chem Eng J 2021;425:130602. https://doi.org/10.1016/j.cej.2021.130602.
[102] Zhang J, Uzun S, Seyedin S, Lynch PA, Akuzum B, Wang Z, et al. Additive-free MXene liquid crystals and fibers. ACS Cent Sci 2020;6:254–65. https://doi.org/10.1021/acscentsci.9b01217.
[103] Nighojkar A, Zimmermann K, Ateia M, Barbeau B, Mohseni M, Krishnamurthy S, et al. Application of neural network in metal adsorption using biomaterials (BMs): a review. Environ Sci Adv 2022. https://doi.org/10.1039/d2va00200k.
[104] He M, Zhang L. Machine learning and symbolic regression investigation on stability of MXene materials. Comput Mater Sci 2021;196:110578. https://doi.org/10.1016/j.commatsci.2021.110578.
[105] Lu S, Zhou Q, Ouyang Y, Guo Y, Li Q, Wang J. Accelerated discovery of stable lead-free hybrid organic-inorganic perovskites via machine learning. Nat Commun 2018;9:3405. https://doi.org/10.1038/s41467-018-05761-w.
[106] Naguib M, Kurtoglu M, Presser V, Lu J, Niu J, Heon M, et al. Two-dimensional nanocrystals produced by exfoliation of Ti3AlC2. Adv Mater 2011;23:4248–53. https://doi.org/10.1002/adma.201102306.
[107] Bajraktarova-Valjakova E, Korunoska-Stevkovska V, Georgieva S, Ivanovski K, Bajraktarova-Misevska C, Mijoska A, et al. Hydrofluoric acid: burns and systemic toxicity, protective measures, immediate and hospital medical treatment. Open Access Maced J Med Sci 2018;6:2257–69. https://doi.org/10.3889/oamjms.2018.429.
[108] Feng A, Yu Y, Wang Y, Jiang F, Yu Y, Mi L, et al. Two-dimensional MXene Ti3C2 produced by exfoliation of Ti3AlC2. Mater Des 2017;114:161–6. https://doi.org/10.1016/j.matdes.2016.10.053.
[109] Halim J, Lukatskaya MR, Cook KM, Lu J, Smith CR, Näslund LÅ, et al. Transparent conductive two-dimensional titanium carbide epitaxial thin films. Chem Mater 2014;26:2374–81. https://doi.org/10.1021/cm500641a.
[110] Wang L, Zhang H, Wang B, Shen C, Zhang C, Hu Q, et al. Synthesis and electrochemical performance of Ti3C2Tx with hydrothermal process. Electron Mater Lett 2016;12:702–10. https://doi.org/10.1007/s13391-016-6088-z.
[111] Xie X, Xue Y, Li L, Chen S, Nie Y, Ding W, et al. Surface Al leached Ti 3 AlC 2 as a substitute for carbon for use as a catalyst support in a harsh corrosive electrochemical system. Nanoscale 2014;6:11035–40. https://doi.org/10.1039/C4NR02080D.
[112] Zhang C, Ma Y, Zhang X, Abdolhosseinzadeh S, Sheng H, Lan W, et al. Two-dimensional transition metal carbides and nitrides (MXenes): synthesis, properties, and electrochemical energy storage applications. Energy Environ Mater 2020;3:29–55. https://doi.org/10.1002/eem2.12058.
[113] Sun Z, Yuan M, Lin L, Yang H, Nan C, Li H, et al. Selective lithiation-expansion-microexplosion synthesis of two-dimensional fluoride-free mxene. ACS Mater Lett 2019;1:628–32. https://doi.org/10.1021/acsmaterialslett.9b00390.
[114] Chen J, Chen M, Zhou W, Xu X, Liu B, Zhang W, et al. Simplified synthesis of fluoride-free Ti3C2Tx via electrochemical etching toward high-performance electrochemical capacitors. ACS Nano 2022;16:2461–70. https://doi.org/10.1021/acsnano.1c09004.
[115] Yin T, Li Y, Wang R, Al-Hartomy OA, Al-Ghamdi A, Wageh S, et al. Synthesis of Ti3C2Fx MXene with controllable fluorination by electrochemical etching for lithium-ion batteries applications. Ceram Int 2021;47:28642–9. https://doi.org/10.1016/j.ceramint.2021.07.023.
[116] Venkateshalu S, Grace AN. MXenes—a new class of 2D layered materials: synthesis, properties, applications as supercapacitor electrode and beyond. Appl Mater Today 2020;18:100509. https://doi.org/10.1016/j.apmt.2019.100509.
[117] Li X, Li M, Yang Q, Liang G, Huang Z, Ma L, et al. In situ electrochemical synthesis of MXenes without acid/alkali usage in/for an aqueous zinc ion battery. Adv Energy Mater 2020;10:2001791. https://doi.org/10.1002/aenm.202001791.
[118] Liu C, Wu H, Wang X, Fan J, Su H, Yang D, et al. Flexible solid-state supercapacitor integrated by methanesulfonic acid/polyvinyl acetate hydrogel and Ti3C2T. Energy Storage Mater 2023;54:164–71. https://doi.org/10.1016/j.ensm.2022.09.037.
[119] Shen Y, Yao A, Li J, Hua D, Tan KB, Zhan G, et al. Dispersive two-dimensional MXene via potassium fulvic acid for mixed matrix membranes with enhanced organic solvent nanofiltration performance. J Membr Sci 2023;666:121168. https://doi.org/10.1016/j.memsci.2022.121168.
[120] Wang H, Wu X. High capacitance of dipicolinic acid-intercalated MXene in neutral water-based electrolyte. Chem Eng J 2020;399:125850. https://doi.org/10.1016/j.cej.2020.125850.
[121] Li Y, Shao H, Lin Z, Lu J, Liu L, Duployer B, et al. A general Lewis acidic etching route for preparing MXenes with enhanced electrochemical performance in non-aqueous electrolyte. Nat Mater 2020;19:894–9. https://doi.org/10.1038/s41563-020-0657-0.
[122] Thomas T, Pushpan S, Aguilar Martínez JA, Torres Castro A, Pineda Aguilar N, Álvarez-Méndez A, et al. UV-assisted safe etching route for the synthesis of Mo2CTx MXene from Mo–In–C non-MAX phase. Ceram Int 2021;47:35384–7. https://doi.org/10.1016/j.ceramint.2021.08.342.
[123] Mei J, Ayoko GA, Hu C, Sun Z. Thermal reduction of sulfur-containing MAX phase for MXene production. Chem Eng J 2020;395:125111. https://doi.org/10.1016/j.cej.2020.125111.
[124] Yan F, Zhang C, Wang H, Zhang X, Zhang H, Jia H, et al. A coupled conductor of ionic liquid with Ti 3 C 2 MXene to improve electrochemical properties. J Mater Chem 2021;9:442–52. https://doi.org/10.1039/D0TA09712H.
[125] Pang S-Y, Wong Y-T, Yuan S, Liu Y, Tsang M-K, Yang Z, et al. Universal strategy for HF-free facile and rapid synthesis of two-dimensional MXenes as multifunctional energy materials. J Am Chem Soc 2019;141:9610–6. https://doi.org/10.1021/jacs.9b02578.
[126] Natu V, Pai R, Sokol M, Carey M, Kalra V, Barsoum MW. 2D Ti3C2Tz MXene synthesized by water-free etching of Ti3AlC2 in polar organic solvents. Chem 2020;6:616–30. https://doi.org/10.1016/j.chempr.2020.01.019.
[127] Jawaid A, Hassan A, Neher G, Nepal D, Pachter R, Kennedy WJ, et al. Halogen etch of Ti 3 AlC 2 MAX phase for MXene fabrication. ACS Nano 2021;15:2771–7. https://doi.org/10.1021/acsnano.0c08630.
[128] Xiu L-Y, Wang Z-Y, Qiu J-S. General synthesis of MXene by green etching chemistry of fluoride-free Lewis acidic melts. Rare Met 2020;39:1237–8. https://doi.org/10.1007/s12598-020-01488-0.
[129] Thapaliya BP, Jafta CJ, Lyu H, Xia J, Meyer HM, Paranthaman MP, et al. Fluorination of MXene by elemental F 2 as electrode material for lithium-ion batteries. ChemSusChem 2019;12:1316–24. https://doi.org/10.1002/cssc.201900003.
[130] Habib T, Zhao X, Shah SA, Chen Y, Sun W, An H, et al. Oxidation stability of Ti3C2Tx MXene nanosheets in solvents and composite films. Npj 2D Mater Appl 2019;3:8. https://doi.org/10.1038/s41699-019-0089-3.
[131] Chae Y, Kim SJ, Cho S-Y, Choi J, Maleski K, Lee B-J, et al. An investigation into the factors governing the oxidation of two-dimensional Ti 3 C 2 MXene. Nanoscale 2019;11:8387–93. https://doi.org/10.1039/C9NR00084D.
[132] Cheng H, Liu Q, Han S, Zhang S, Ouyang X, Wang X, et al. Highly efficient photothermal conversion of Ti3C2T x/ionic liquid gel pen ink for smoothly writing ultrasensitive, wide-range detecting, and flexible thermal sensors. ACS Appl Mater Interfaces 2020;12:37637–46. https://doi.org/10.1021/acsami.0c13215.
[133] Zhao H, Ding J, Zhou M, Yu H. Air-stable titanium carbide MXene nanosheets for corrosion protection. ACS Appl Nano Mater 2021;4:3075–86. https://doi.org/10.1021/acsanm.1c00219.
[134] Conway JW, Madwar C, Edwardson TG, McLaughlin CK, Fahkoury J, Lennox RB, et al. Dynamic behavior of DNA cages anchored on spherically supported lipid bilayers. J Am Chem Soc 2014;136:12987–97. https://doi.org/10.1021/ja506095n.
[135] Lin H, Gong K, Hykys P, Chen D, Ying W, Sofer Z, et al. Nanoconfined deep eutectic solvent in laminated MXene for efficient CO2 separation. Chem Eng J 2021;405:126961. https://doi.org/10.1016/j.cej.2020.126961.
[136] Kim J, Yoon Y, Kim SK, Park S, Song W, Myung S, et al. Chemically stabilized and functionalized 2D-MXene with deep eutectic solvents as versatile dispersion medium. Adv Funct Mater 2021;31:2008722. https://doi.org/10.1002/adfm.202008722.
[137] Wu J, Wang Y, Zhang Y, Meng H, Xu Y, Han Y, et al. Highly safe and ionothermal synthesis of Ti3C2 MXene with expanded interlayer spacing for enhanced lithium

storage. J Energy Chem 2020;47:203–9. https://doi.org/10.1016/j.jechem.2019.11.029.
[138] Zhang M, Liang R, Yang N, Gao R, Zheng Y, Deng Y, et al. Eutectic etching toward in-plane porosity manipulation of Cl-terminated MXene for high-performance dual-ion battery anode. Adv Energy Mater 2022;12:2102493. https://doi.org/10.1002/aenm.202102493.
[139] Rozmysłowska-Wojciechowska A, Wojciechowski T, Ziemkowska W, Chlubny L, Olszyna A, Jastrzębska AM. Surface interactions between 2D Ti3C2/Ti2C MXenes and lysozyme. Appl Surf Sci 2019;473:409–18. https://doi.org/10.1016/j.apsusc.2018.12.081.
[140] Li M, Lu J, Luo K, Li Y, Chang K, Chen K, et al. Element replacement approach by reaction with Lewis acidic molten salts to synthesize nanolaminated MAX phases and MXenes. J Am Chem Soc 2019;141:4730–7. https://doi.org/10.1021/jacs.9b00574.
[141] Srimuk P, Kaasik F, Krüner B, Tolosa A, Fleischmann S, Jäckel N, et al. MXene as a novel intercalation-type pseudocapacitive cathode and anode for capacitive deionization. J Mater Chem 2016;4:18265–71. https://doi.org/10.1039/C6TA07833H.
[142] Chen X, Wang S, Shi J, Du X, Cheng Q, Xue R, et al. Direct laser etching free-standing MXene-MoS 2 film for highly flexible micro-supercapacitor. Adv Mater Interfac 2019;6:1901160. https://doi.org/10.1002/admi.201901160.
[143] Gavriel B, Shpigel N, Malchik F, Bergman G, Turgeman M, Levi MD, et al. Enhanced performance of Ti3C2Tx (MXene) electrodes in concentrated ZnCl2 solutions: a combined electrochemical and EQCM-D study. Energy Storage Mater 2021;38:535–41. https://doi.org/10.1016/j.ensm.2021.03.027.
[144] Zhou Y, Maleski K, Anasori B, Thostenson JO, Pang Y, Feng Y, et al. Ti3C2Tx MXene-reduced graphene oxide composite electrodes for stretchable supercapacitors. ACS Nano 2020;14:3576–86. https://doi.org/10.1021/acsnano.9b10066.
[145] Anasori B, Lukatskaya MR, Gogotsi Y. 2D metal carbides and nitrides (MXenes) for energy storage. Nat Rev Mater 2017;2:16098. https://doi.org/10.1038/natrevmats.2016.98.
[146] Zada S, Dai W, Kai Z, Lu H, Meng X, Zhang Y, et al. Algae extraction controllable delamination of Vanadium carbide nanosheets with enhanced near-infrared photothermal performance. Angew Chem Int Ed 2020;59:6601–6. https://doi.org/10.1002/anie.201916748.
[147] Song M, Pang SY, Guo F, Wong MC, Hao J. Fluoride-free 2D niobium carbide MXenes as stable and Biocompatible nanoplatforms for electrochemical biosensors with ultrahigh sensitivity. Adv Sci 2020;7:1–8. https://doi.org/10.1002/advs.202001546.
[148] Xue Z, Zeng S, Hao J. Non-invasive through-skull brain vascular imaging and small tumor diagnosis based on NIR-II emissive lanthanide nanoprobes beyond 1500 nm. Biomaterials 2018;171:153–63. https://doi.org/10.1016/j.biomaterials.2018.04.037.
[149] Kim H, Wang Z, Alshareef HN. Nano Energy 2019;60:179–97. https://doi.org/10.1016/j.nanoen.2019.03.020. 10.1016/j.nanoen.2019.03.020.
[150] Nie Y, Liang Z, Wang P, Ma Q, Su X. MXene-derived quantum Dot@Gold nanobones heterostructure-based electrochemiluminescence sensor for triple-negative breast cancer diagnosis. Anal Chem 2021;93:17086–93. https://doi.org/10.1021/acs.analchem.1c04184.
[151] Zhu H, Jiang D, Zhu J-J. High-resolution imaging of catalytic activity of a single graphene sheet using electrochemiluminescence microscopy. Chem Sci 2021;12:4794–9. https://doi.org/10.1039/D0SC06967A.
[152] Xue Q, Zhang H, Zhu M, Pei Z, Li H, Wang Z, et al. Photoluminescent Ti3C2 MXene quantum dots for multicolor cellular imaging. Adv Mater 2017;29:1604847. https://doi.org/10.1002/adma.201604847.
[153] Rastogi S, Kandasubramanian B. Progressive trends in heavy metal ions and dyes adsorption using silk fibroin composites. Environ Sci Pollut Res 2020;27:210–37. https://doi.org/10.1007/s11356-019-07280-7.
[154] Gore PM, Naebe M, Wang X, Kandasubramanian B. Progress in silk materials for integrated water treatments: fabrication, modification and applications. Chem Eng J 2019;374:437–70. https://doi.org/10.1016/j.cej.2019.05.163.
[155] Udayakumar KV, Gore PM, Kandasubramanian B. Foamed materials for oil-water separation. Chem Eng J Adv 2021;5:100076. https://doi.org/10.1016/j.ceja.2020.100076.
[156] Gore P, Khraisheh M, Kandasubramanian B. Nanofibers of resorcinol–formaldehyde for effective adsorption of as (III) ions from mimicked effluents. Environ Sci Pollut Res 2018;25:11729–45. https://doi.org/10.1007/s11356-018-1304-z.
[157] Rajhans A, Gore PM, Siddique SK, Kandasubramanian B. Ion-imprinted nanofibers of PVDF/1-butyl-3-methylimidazolium tetrafluoroborate for dynamic recovery of europium (III) ions from mimicked effluent. J Environ Chem Eng 2019;7:103068. https://doi.org/10.1016/j.jece.2019.103068.
[158] Pillai A, Kandasubramanian B. Carbon xerogels for effluent treatment. J Chem Eng Data 2020;65:2255–70. https://doi.org/10.1021/acs.jced.0c00092.
[159] Chen S, Liu H. Self-reductive palladium nanoparticles loaded on polydopamine-modified MXene for highly efficient and quickly catalytic reduction of nitroaromatics and dyes. Colloids Surfaces A Physicochem Eng Asp 2022;635:128038. https://doi.org/10.1016/j.colsurfa.2021.128038.
[160] Li K, Jiao T, Xing R, Zou G, Zhou J, Zhang L, et al. Fabrication of tunable hierarchical MXene@AuNPs nanocomposites constructed by self-reduction reactions with enhanced catalytic performances. Sci China Mater 2018;61:728–36. https://doi.org/10.1007/s40843-017-9196-8.
[161] Li K, Liao J, Huang S, Lei Y, Zhang Y, Zhu W. Enhanced catalytic properties of cobaltosic oxide through constructing MXene-supported nanocomposites for ammonium perchlorate thermal decomposition. Appl Surf Sci 2021;570:151224. https://doi.org/10.1016/j.apsusc.2021.151224.
[162] Ye W, Yu J, Zhou Y, Gao D, Wang D, Wang C, et al. Green synthesis of Pt-Au dendrimer-like nanoparticles supported on polydopamine-functionalized graphene and their high performance toward 4- nitrophenol reduction. Appl Catal B Environ 2016;181:371–8. https://doi.org/10.1016/j.apcatb.2015.08.013.
[163] Seyedin S, Yanza ERS, Razal JM. Knittable energy storing fiber with high volumetric performance made from predominantly MXene nanosheets. J Mater Chem 2017;5:24076–82. https://doi.org/10.1039/C7TA08355F.
[164] Yang Q, Xu Z, Fang B, Huang T, Cai S, Chen H, et al. MXene/graphene hybrid fibers for high performance flexible supercapacitors. J Mater Chem 2017;5:22113–9. https://doi.org/10.1039/C7TA07999K.